FACULDADE DE ENGENHARIA DA UNIVERSIDADE DO PORTO

Automatic Detection of Focal Cortical Dysplasias on Magnetic Resonance Images of Patients with Refractory Focal Epilepsy

João Mendo Gatta

Master's Program in Biomedical Engineering

Supervisor: Professor Paulo Aguiar

Co-supervisor: Dra. Catarina Pinto

Co-supervisor: Dr. Joel Freitas

July 30, 2024

Automatic Detection of Focal Cortical Dysplasias on Magnetic Resonance Images of Patients with Refractory Focal Epilepsy

João Mendo Gatta

Master's Program in Biomedical Engineering

July 30, 2024

Resumo

A epilepsia é uma doença do cérebro que afecta milhões de pessoas com convulsões debilitantes, que podem causar danos irreparáveis no tecido neural, especialmente quando ocorre durante a infância, afetar a vida social e profissional, prejudicar a autoestima e até, levar à morte.
A humanidade tem lidado com a epilepsia há milhares de anos, inicialmente com suspeitas de origem mitológica e consequente condenação dos afectados, e agora com uma razoável compreensão das suas causas e um procedimento clínico detalhado. Apesar disso, existem ainda algumas dificuldades a ultrapassar, especialmente no que respeita aos doentes cuja frequência dos ataques epiléticos não é controlável apenas com medicação anti-convulsiva. Estes doentes têm epilepsia refractária, uma forma da doença que normalmente é tratada através de cirurgia ressectiva. Uma razão comum subjacente à natureza refractária de um determinado caso de epilepsia é a presença de uma Displasia Cortical Focal (DCF). Trata-se de uma malformação do tecido cerebral que pode induzir uma atividade eléctrica nos neurónios inadequada, conduzindo assim a convulsões. A sua correcta identificação e delimitação num determinado exame de Ressonância Magnética, o diagnóstico típico utilizado, é crucial para o planeamento cirúrgico adequado. Durante a cirurgia de ressecção, o objetivo é remover a maior quantidade possível de tecido considerado como uma DCF, preservando o tecido saudável circundante. Infelizmente, cerca de um terço de todos os DCFs não são detectados durante a inspeção visual, mesmo por neurorradiologistas especializados. Foram propostos vários métodos de processamnto computacional para ajudar os clínicos, com resultados muito promissores, mas a sua integração no fluxo de trabalho clínico diário continua a ser um grande obstáculo a ultrapassar. Estes softwares propostos têm normalmente uma curva de aprendizagem acentuada e requerem alguns conhecimentos técnicos para serem implementados. Deste desafio surge a necessidade de desenvolver uma Interface Gráfica do Utilizador (GUI, em inglês), como ponte entre os métodos assistidos por computador, clinicamente relevantes mas difíceis de implementar, e os clínicos que mais precisam deles, beneficiando os doentes de epilepsia com uma maior probabilidade de um resultado cirúrgico bem sucedido.
O objetivo proposto foi alcançado, com uma GUI que foi desenvolvida com um ênfase na usabilidade, intuitividade e eficiência, automatizando a execução de um algoritmo automático de deteção de DCFs e fornecendo funcionalidades adicionais, úteis no dia-a-dia clínico.

Abstract

Epilepsy is a brain disease that affects millions of people with debilitating seizures, that can cause irreparable neural tissue damage, specially when the onset occurs during childhood, can affect their social and professional lives, damage their self-esteem and ultimately, lead to death.
Humanity has dealt with epilepsy for thousands of years, at first with suspicions of mythological origin and subsequent condemnation of those afflicted, and now with a reasonable understanding of its causes and a detailed clinical procedure. Regardless, there are still some difficulties to overcome, specially regarding patients that do not achieve a manageable level of seizure frequency with antiseizure medication alone. These patients have refractory epilepsy, a form of the disease that usually is dealt with through resective surgery. A common underlying reason for the refractory nature of a given epilepsy case is the presence of a Focal Cortical Dysplasia (FCD). These are brain tissue malformations that can induce improper eletrical activity in the neurons thus leading to seizures. Their proper identification and delineation in a given Magnetic Resonance Imaging scan, the typical diagnostic used, is crucial for the proper surgical planning. During resective surgery, the aim is to remove as much tissue considered to be an FCD as possible while preserving the surrounding healthy tissue. Unfortunately, about a third of all FCDs are missed during visual inspection, even by expert neuroradiologists. Several computer-based methods have been proposed to aid clinicians, with very promising results but their integration within the typical clinical workflow still remains a big obstacle to overcome. These proposed software typically carry a steep learning curve and require some technical knowledge to implement. From this challenge the need to develop a Graphical User Interface (GUI) emerges, as a bridge between the clinically relevant but hard to implement computer-assisted methods and the clinicians that need them the most, benefiting epilepsy patients with a higher probability of a successful surgical outcome.
The proposed goal was achieved, with a GUI that was developed with a large focus on usability, intuitiveness and efficiency, automating the execution of an automatic FCD detection algorithm and providing additional features, useful in the daily clinical workflow.

Agradecimentos

Ao meu orientador e amigo Dr. Paulo Aguiar, pela postura de apoio e dedicação incansáveis com que me orientou e com que lidera o NCN. Pela oportunidade que me deu de concretizar o meu sonho de transicionar de área do saber, integrando-me numa equipa fenomenal, tanto do ponto de vista científico como humano. Passei por ocasiões tumultuosas durante esta etapa da minha vida e sem a tua mentoria e o teu entendimento, esta dissertação não seria uma realidade. Obrigado Paulo!
Aos restantes membros do NCN, gostava de agradecer pela vossa capacidade de me terem feito sentir parte da família logo no primeiro dia em que pus os pés no i3s. Desde as conversas incríveis à hora de almoço (sempre na esplanada, quer com frio e chuva quer com calor e céu azul), às risadas nas reuniões semanais, aos jantares de grupo e ao apoio constante durante a escrita desta dissertação.
À minha mãe, por ser a pessoa mais lutadora que conheço e por ter sido o meu pilar de apoio nos momentos de maior dúvida. Sem a tua ajuda, e paciência interminável para me ouvires a refilar, este trabalho não seria possível.
Ao meu pai, pela infinidade de conversas e debates interessantes, pelos conselhos de vida e por nunca duvidar de mim, mesmo quando as decisões são arriscadas.
Ao "Gang do Cachalote", grupo de amigos dos Açores, pelos serões de conversas e risadas constantes com que preencho muitos dos meus dias. A definição de "amigos para a vida" e a minha maior fonte de alívio de stress.
Às novas amizades que o Porto me trouxe, quer as formadas nos primeiros dias em que esta cidade me acolheu, quer as mais recentes. Foi aqui no Porto que conheci algumas das pessoas mais incríveis, com as quais espero manter contacto sempre.

Obrigado a todos!

João Mendo Gatta

"There are decades where nothing happens; and there are weeks where decades happen."

Vladimir Lenin

Contents

List of Figures

Abreviaturas e Símbolos

ANOVA	Analysis of variance
ANTs	Advanced Normalization Tools
CAT	Computational Anatomical Toolbox
CNN	Convolutional Neural Network
DICOM	Digital Imaging and Communications in Medicine
DL	Deep Learning
EEG	Electroencephalogram
FCD	Focal Cortical Dysplasia
FDR	False Discovery Rate
FGM	Finite Gaussian Mixture
FLAIR	Fluid Attenuated Inversion Recovery
FWE	Family-wise Error
GLM	General Linear Model
GUI	Graphical User Interface
HMRF	Hidden Markov Random Field
IBE	International Bureau for Epilepsy
ILAE	International League Against Epilepsy
MELD	Multi-centre Epilepsy Lesion Detection
ML	Machine Learning
MNI	Montreal Neurological Institute
MRI	Magnetic Resonance Imaging
NIfTI	Neuroimaging Informatics Technology Initiative
PACS	Picture Archiving and Communications Systems
PET	Positron Emission Tomography
ROI	Region of Interest
SBM	Surface-based Morphometry
SPECT	Single-photon emission computed tomography
SPM	Statistical Parametric Mapping
SUDEP	Sudden Unexpected Death in Epilepsy
SVM	Support Vector Machine
VBM	Voxel-based Morphometry
WISC-IV	Wechsler Intelligence Scale for Children, Fourth Edition

Chapter 1

Introduction

In 2015, the International Day of Epilepsy was established by the International Bureau for Epilepsy (IBE) and the International League Against Epilepsy (ILAE), the two best-known authorities in this field. Celebrated annually on the second Monday in February, it serves as a reminder of the growing prevalence of epilepsy, its impact on the lives of those afflicted, and the stigmatisation, discrimination, and human rights violations that people with epilepsy still face. According to the World Health Organisation's Epilepsy Fact Sheet 2024, around 50 million people worldwide are affected by this chronic, non-communicable brain disease, with 5 million new diagnoses being made every year.

Epilepsy patients exhibit well-known symptoms such as seizures, unusual behavior and sometimes loss of awareness. A major problem regarding seizures is their variability in frequency and intensity. This unpredictability contributes to the need for these patients to be regularly hospitalized, as many injuries can occur in their daily lives due to unfortunate seizure timing. In more severe cases, the constant anticipation of the next seizure, along with the side effects of antiseizure medications, can negatively impact the mental health of the patients, leading to anxiety, depression and cognitive impairment. All of these difficulties contribute to a feeling of social exclusion and lower self-esteem(1).

One of the most alarming and tragic complications associated with epilepsy is sudden unexpected death in epilepsy (SUDEP). SUDEP is defined as the sudden, unexpected, non-traumatic, non-drowning death of a person with epilepsy in which autopsy does not reveal a structural or toxicological underlying cause. While the exact mechanisms behind SUDEP remain unclear, it

is thought to be related to seizure-related respiratory or cardiac dysfunction. SUDEP is the most common cause of epilepsy-related deaths, underlining the importance of effective seizure management and monitoring to reduce this risk(2).

1.1 Context and Motivation

In the clinical classification of epilepsy patients, a key divide is made between those who achieve sustained seizure freedom through antiseizure medications, representing around two-thirds of the patient population, and the remaining third, where persistent seizures remain even when adequate medication trials are tested(3). The latter group is characterized as having refractory epilepsy and faces additional complications, such as higher rates of anxiety and depression which in turn have been proved to worsen seizures(4). Additionally, 30-40% of children with refractory epilepsy have a co-existing intellectual disability(5) and, in the working population, there is a significant decrease in wage-based productivity almost reaching the losses of the diabetes, depression, anxiety and asthma populations combined(6).

The persistent seizures that characterize refractory epilepsy may originate from a specific area within one of the brain hemispheres, thus being classified as focal, or they may have multiple origins spread across both hemispheres, known as generalized. Although both seizure types are regularly diagnosed in the same patient, indicating that this seemingly binary classification exists more in a spectrum(7), seizures originating from a specific location, defined as a focal area, are more prevalent(8). Untreated epilepsy has been shown to cause structural damage to the brain, which in turn increases the frequency of seizures. This characteristic, as well as the other complications already mentioned, makes it imperative that the clinical assessment of a particular patient is done in a timely manner. If the origin of the seizures is sufficiently localized and the antiseizure medications are not adequately alleviating the onset of seizures, then the patient is considered to have refractory focal epilepsy.

The next clinical step is to determine if the patient is eligible for a surgical procedure of the focal area or if the focus should be on palliative care. The latter being comprised of several techniques such as subpial transections, ketogenic diet, vagal nerve stimulations and corpus callosotomy with each technique being best suited for a specific epilepsy syndrome(3). If surgery is considered to be the next clinical step, then a detailed planning is required, to ensure the best possible outcome

for the patient. The first part of this planning involves acquiring information regarding the medical history of the patient and their seizures, obtained via a thorough neurological examination, as well as a set of neuroimaging studies, typically consisting of Magnetic Resonance Imaging (MRI) and Positron Emission Tomography (PET) scans. The efficacy of this protocol impacts the surgery greatly, given the improvement it provides to the important procedure of localizing the origin of the seizures and the surrounding eloquent areas of the brain. This theoretical area is called the epileptogenic area and it is the focus of the subsequent resective surgery which aims to remove the least amount of brain tissue required to cease seizure onset, whilst avoiding eloquent cortex(9). Frequently linked with this region, especially in pediatric patients, are Focal Cortical Dysplasias (FCDs)(10).

FCDs are a form of developmental brain abnormality characterized by atypical growth of neurons and supportive cells in a particular brain region, resulting in focal seizures originating from that area in 75% of all FCD cases(11). The detection of FCDs can be facilitated through MRI scans, and if detected, this data is factored in during the preparation for resective surgery. Occasionally, the epileptogenic zone may coincide with the FCD, in which scenario, the surgical team will strive to excise as much of the FCD as feasible while safeguarding the neighboring brain tissue.

From this direct relationship between FCDs and focal seizures, arises the critical need to correctly identify and segment them in MRI images, which is paramount for adequately planning surgical interventions. The failure to detect a lesion in MRI has been associated with surgical failure in large cohorts of patients(12). Unfortunately, due to several factors such as MRI image quality limitations, acquisition protocols, the anatomical characteristics of the FCD and the expert clinician's time constraints, up to 30% of postoperative pathologically verified FCDs are not detected during surgery planning(13). To help overcome this challenge a wide range of computer-assisted methods for FCD detection have been developed, most of which fall into the categories of Brain Morphometry and Machine Learning. Although several of these implementations perform at a medically meaningful level, deploying them in the daily clinical practise has proven to be very challenging(14)(15). The lack of widely distributed, ready-to-use solutions halts the necessary progress in FCD detection and prevents a higher number of epilepsy patients from achieving a seizure-free clinical outcome.

1.2 Objectives

In direct collaboration with clinicians from the Neuroradiology and Neurophysiology departments of Hospital Santo António - Centro Hospitalar Universitário do Porto and inserted in the context of the Neuroengineering and Computational Neuroscience (NCN) group at the Institute for Research and Innovation in Health (i3s) , **the main objective of this dissertation is to implement a ready-to-use Graphical User Interface (GUI) that allows for the adoption of an open-source FCD detection Machine Learning algorithm into the daily clinical workflow.** The developed GUI aims to bridge the gap between the chosen FCD detection method and its usability by clinicians, providing an intuitive, and quick procedure to run a prediction on any relevant patient. It also aims to provide an elegant and reliable solution to visualize MRI scans, with basic image manipulation features as well as file type conversions.

1.3 Challenges

Adapting an existing ML model to a specific dataset inevitably poses some challenges, especially regarding potential variability between the data used for training and the data the model is going to be used on in the clinic. This typically results in a worse performing algorithm that could become clinically irrelevant(15). One possible strategy to tackle this issue, is to develop a standalone algorithm, trained with a dataset that is representative of the data to be inferred upon. This approach demands a sufficiently sized dataset, that allows the ML model to learn the specific characteristics of the data with enough examples to achieve a satisfactory performance. When dealing with MRI scans, the inter-subject variability is quite significant, specially in the case of epilepsy surgery where most patients are younger than 18 years old, so their brain is still undergoing significant structural changes(16) and also movement artifacts are more prevalent(17), both negatively impacting the performance of the ML model.(18). Since acquiring a large enough dataset to surpass these obstacles was not feasible and given the recent increase in academic interest for automatic FCD detection(19), a decision to survey the available open-source methods and choose the most adequate solution was made.

Chapter 2

Epilepsy

"His neck turning left, hands and feet are tense, and his eyes wide open, and from his mouth froth is flowing without him having any consciouness"(20) This ancient inscription, discovered on a stone tablet dating back 4000 years, provides a detailed account of an individual experiencing a convulsion or seizure, which is the most common and distinctive symptom of epilepsy. Epilepsy is a condition that has plagued humanity for a significant period of time, but it was only in 1909 that the ILAE, one of the foremost global authorities on epilepsy, was established. The primary objective of the ILAE is to enhance the quality of life for individuals with epilepsy through extensive research. As such, it serves as the primary source for the most current and comprehensive information on the definitions and classifications of various aspects of epilepsy. According to the ILAE, epilepsy is defined by the presence of at least one of the following conditions in a patient: two or more unprovoked seizures occurring more than 24 hours apart, one unprovoked seizure with a recurrence probability of at least 60% over a period of 10 years, or a diagnosis of an epilepsy syndrome.

2.1 Historical Context

2.1.1 Primordial Views on Epilepsy

Epilepsy is one of the oldest documented neurological disorders, with descriptions dating back to ancient Mesopotamia, around 2000 BCE. A millennium later attempts to document epilepsy's symptomatology were found in a Babylonian medical text known as the "Sakikku." This text attributed the characteristic seizures to demonic or divine intervention, viewing them as forms of

punishment or reward, respectively. Although the causes of the disease were far from understood, observations of different seizure types and their respective health outcomes were written in formal language to standardize relevant nomenclature and contribute to a possible cure(20). Around 1790 BCE, the symptoms of epilepsy were described in detail in The Code of Hammurabi, along with a law that allowed slave owners to return a slave to the previous master if he/she had an epileptic event within a month of being purchased(21). Ninety years later, in Egypt, a particularly poignant revelation was made, when a man with a large wound in his head began having seizures whenever some pressure was applied to the afflicted area(22). This is perhaps the first written observation about the role of the brain in the onset of seizures. Unfortunately, this observation did not lead to a formal investigation into the origins of epilepsy for another 1200 years. It was Greek physician Hippocrates, considered the father of modern Medicine, who theorized that epilepsy originated in the brain, stating: "But the brain is the cause of this affection, as it is of other very great diseases, and in what manner and from what cause it is formed, I will now plainly declare"(23). This excerpt comes from the book Hippocratic Corpus, in which several medical conditions are described and a refusal of their mythological origin is proposed, being replaced by a more systematic, perhaps scientific, analysis of the ailments.

2.1.2 Modern era

The new perspective that Hippocrates offered was not widely adopted and the perceived superstitious nature of epilepsy persisted for more than 2000 years. Only during the 18th century were Hippocrates' views of epilepsy re-considered, specifically by Samuel Tissot, a Swiss physician, who in his 1770 book Traité d l'épilepsie, attempted to arrive at a plausible disease cause with a focus on the nervous system, alongside a detailed symptomology and treatment plan(24). Tissot's book and the values imposed on Medicine during the Enlightenment period propelled the interest to study epilepsy more deeply and aided in the reduction of the social stigma and ostracism that the typical epilepsy patient was a victim of. During the following 19th century, several types of seizures were described, like the grand mal, petit mal and Jacksonian seizures, all of which are still clinically relevant. The late 19th and early 20th centuries also saw an increase in epilepsy research, made possible, in large part, due to the creation of the Electroencephalogram (EEG), which made it possible to analyze the brain's electrical activity, and crucial insights into

the brain's anatomy such as the first microscopic description of the neurons, made by Santiago Ramón y Cajal, which awarded him a Nobel Prize in Medicine(25). These findings allowed for crucial experiments that characterized the 20th-century research on epilepsy, such as confirming the relationship between abnormal electrical activity in the brain and seizures, done via experimentally inducing them in dogs, a procedure done by the Russian physiologist Kaufman in 1912; the contributions made by German neurologist Berger, namely his detection of EEG changes in the brain after a generalized tonic-clonic seizure(26) or establishing the correlation between specific EEG readings and the underlying seizures, work done in 1935-1941 by Frederic Andrews Gibbs, his wife Erna Leonhardt-Gibbs and William Gordon Lennox that resulted in the publication of "Atlas of Electroencephalography", a seminal contribution to the field. The trend of using EEG to map the electrical signals of the brain continued with Henri Jean Paul Gastaut, a French neurologist, who described several human EEG electrical brain patterns and 2 epilepsy syndromes that were named after him: the Gastaut syndrome and, built on previous work from Lennox, the Lennox-Gastaut syndrome. From the 1950s onwards, the clinical repercussions of these developments in the epilepsy research field, were starting to become more noticeable, with the adoption of new surgical techniques, the introduction of the first antiseizure medications and symptom management techniques such as vagal nerve stimulation, and ketogenic diet(26). Alongside these clinical improvements, an effort was made to create relevant institutions that could tackle the negative, pre-conceived notions surrounding epilepsy patients, and aid in the standardization of relevant disease terminology. In 1961 the International Bureau for Epilepsy, or IBE, was created and in 1970 the ILAE published the first formal classification of the various epilepsy syndromes. Neuroimaging technology also rapidly improved, with MRI, SPECT, and PET being placed at the forefront of the clinical treatment plan of epilepsy, aiding in the evaluation of pathological causes for the seizures, such as brain tumors, strokes, inflammation and dysplasias.

The intricate history of epilepsy is filled with promising advances and devastating setbacks but the current scenario and attitude towards the disease shows humanity's commitment to the improvement of epilepsy patient's lives, both in regards to the quality of the clinical care provided and the societal perception of the afflicted population.

2.2 Classification of the Epilepsies

Epilepsy is often perceived as a singular disease, but it encompasses a diverse array of syndromes, each with distinct etiologies, seizure types, and associated comorbidities(27).

The initial step in diagnosing epilepsy involves categorizing the seizure type, which falls into three primary groups: focal onset, generalized onset, and unknown onset. Following this, the epilepsy type is determined, which considers the initial diagnosis to better describe the observed symptoms. These categories include focal epilepsy, generalized epilepsy, combined generalized and focal epilepsy, and an unknown category.

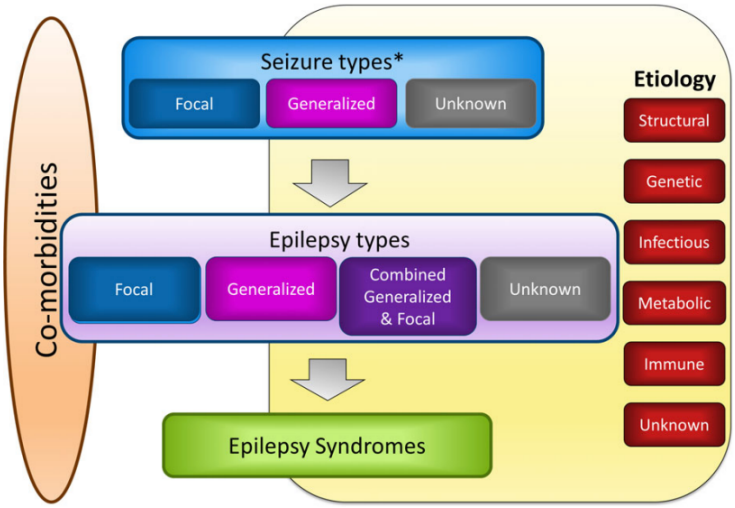

Figure 2.1: How to classify different epilepsies. Adapted from (27)

It is noteworthy that many epilepsy cases present a combination of both focal and generalized seizures. The recognition of this combination in a more recent category reflects actual clinical observations. For patients diagnosed with generalized epilepsy, the following seizure types are typically observed:

1. Absence Seizures - These are characterized by a sudden loss of consciousness, lasting a few seconds to a minute, often with the patient staring blankly into space. Symptoms may include eye blinking, lip smacking, and hand movements, and these seizures are commonly seen in children and adolescents(28).

2. Myoclonic Seizures - Marked by sudden, brief, and jerky movements in the arms, legs, or face, these seizures are frequently associated with juvenile myoclonic epilepsy.(29).

3. Atonic Seizures - Characterized by a sudden loss of muscle tone, these seizures cause the patient to drop their head, arms, or entire body and are also known as "drop attacks," often seen in individuals with Lennox-Gastaut syndrome(30).

4. Tonic Seizures - These involve sudden and sustained muscle contractions, resulting in rigidity and falling, and are typically seen in individuals with tonic epilepsy(31).

5. Tonic-Clonic Seizures - Also known as "grand mal" seizures, these involve a combination of tonic and clonic movements, including muscle stiffness followed by rhythmic muscle contractions. They can occur in individuals with various types of epilepsy(31).

The specific seizure type, combined with the identification of interictal (between seizures) EEG discharges, facilitates the diagnosis of generalized epilepsy.

Focal epilepsy includes both unifocal and multifocal disorders, with seizures originating from one hemisphere. The main seizure types in focal epilepsy are:

1. Focal Aware Seizures: These seizures involve changes in sensation, movements, emotions, or other neurological symptoms confined to a specific brain area, with the individual remaining conscious and aware. Symptoms can include sudden jerking movements, tingling sensations, changes in vision, auditory or olfactory hallucinations, déjà vu experiences, and emotional changes(32).

2. Focal Impaired Awareness Seizures: Similar to focal aware seizures but with a loss of consciousness or awareness during the event. Symptoms may include staring spells, repetitive movements or behaviors, and post-seizure confusion or disorientation(32).

3. Focal Motor Seizures: Characterized by involuntary muscle contractions or movements in a specific body part, such as twitching or jerking of an arm or leg.(33)

4. Focal Non-Motor Seizures: These involve changes in sensory perception, emotion, or autonomic functions, such as changes in taste, smell, or heart rate(34).

5. Focal to Bilateral Tonic-Clonic Seizures: These seizures begin as focal seizures but rapidly spread to involve both sides of the brain, resulting in tonic-clonic (grand mal) seizures, which can cause loss of consciousness and convulsions(34).

The ideal diagnostic approach involves identifying the specific epilepsy syndrome based on the presented symptoms. However, this is not always possible due to the challenges in determining the underlying etiology. As a result, many cases are diagnosed based solely on seizure type. A more precise diagnosis can be achieved when seizure types, imaging data, EEG information, and relevant patient details align with a recognized epilepsy syndrome. Within generalized epilepsy, a significant subgroup is Idiopathic Generalized Epilepsies. This group includes Childhood Absence Epilepsy, Juvenile Absence Epilepsy, Juvenile Myoclonic Epilepsy, and Generalized Tonic-Clonic Seizures Alone. These syndromes often exhibit a strong genetic predisposition. Research, particularly studies comparing epilepsy prevalence among family members and twins, continues to validate this classification(27). For focal epilepsy, the most prevalent subgroup is Self-limited Focal Epilepsies. These are categorized based on the anatomical location of the focal point and include self-limited centrotemporal, occipital, frontal, temporal, and parietal epilepsies.

2.3 Disease Origin

Epilepsy has varying clinical manifestations and underlying biological origins. Since seizures are epilepsy's defining symptom, and the aim of the clinical interventions, determining a disease origin typically revolves around focusing on the seizures, to find the anatomical locations where the onset of the abnormal electrical activity occurs, through several electrophysiology and neuroimaging techniques. This allows clinicians to characterize each case within the following categories, as standardized by the ILAE in 2017(27):

1. Genetic - This category is typically attributed to a given patient depending on the presence of epilepsy in their family history. Our understanding of the genes most responsible for epilepsy is still very limited and most syndromes still lack a listing of their genetic correlate foundations.

2. Structural - A given epilepsy case receives this classification when the information retrieved from diagnostic protocols such as MRI scans is deemed enough to explain the source of the seizures with an underlying structural abnormality. Typical origins for the abnormalities include trauma, strokes, infection, and genetic malformations.

3. Infectious - Originating from medical conditions such as malaria, cerebral toxoplasmosis and neurocysticercosis, it is the most prevalent epilepsy etiology. Typically associated with this subset of the patient population, the existence of a structural abnormality is found, normally caused by the infection.

4. Metabolic - Any epilepsy case with seizures that occur due to a disruption in the normal metabolic processes falls under this category. The most common diseases that originate this type of seizure are aminoacidopathies, porphyria, and uremia.

5. Immune - One of the hardest subtypes to diagnose, it is characterized by an inflammation of the central nervous system.

6. Unknown - Restricted to cases where the seizure onset location and type are known, but the fundamental cause is not.

2.4 Focal Cortical Dysplasia

Of the genetic malformations present in epilepsy of structural etiology, a significant one, responsible for most medically refractory epilepsy cases are FCDs(10). They were first discovered in 1971(35), and have been the focus of many studies ever since. According to an ILAE report(36), FCD is used to mean multiple brain lesions including cortical dyslamination, cytoarchitectural lesions, and abnormalities in white matter. This ambiguity in definition isn't clinically helpful so, in 2010, and building on previous attempts to organize these definitions, the ILAE developed a categorization system that divides FCDs into these subtypes:

1. FCD Type I - Brain tissue malformation that displays atypical cortical layering, compromising the normal maturation of neurons and their radial migration (FCD Type Ia). Also can present an unusual six-layer composition of the surrounding neocortex (FCD Type Ib).

   (a) FCD Type Ia - Characterized by having "microcolumns", which is the description used for vertical stacks of more than eight neurons. Typically verified histopathological it inflicts cognitive disabilities and frequent seizures on the patients.

   (b) FCD Type Ib - Presents abnormal cortical laminar organization, with the normal six-layer structure being replaced by a new, malformed arrangement. Commonly associated with cognitive impairments and intractable epilepsy.

   (c) FCD Type Ic - Attributed to patients who present both aforementioned subtypes, with radial and tangential cortical malformations. Considered to be the most clinically challenging form of FCD Type I, with most patients having uncontrollable seizures and a strong cognitive impairment.

2. FCD Type II - Characterized by cytologic abnormalities and a disruption of the cortical lamination. The key difference between Type II and Type I is the dissolution of the clear border between cortical layers in the former.

   (a) FCD Type IIa - This subtype is characterized by the presence of dysmorphic neurons that are enlarged, misaligned, and have an accumulation of neurofilament proteins. It is distinguished by the absence of balloon cells and a merging of cortical layers, which makes them difficult to differentiate.

   (b) FCD Type IIb - The presence of dysmorphic neurons and balloon cells, along with abnormal cortical layer organization and heterotopic neurons in the white matter, characterizes this condition. Balloon cells, identified using H&E stain, exhibit large cell bodies and a transparent, glass-like cytoplasm. On T1-weighted MRI scans, subcortical white matter demyelination often causes blurring between gray and white matter, resulting in increased cortical thickness.

3. FCD Type III - This subtype has similar characteristics with FCD Type II but has an adjacent, secondary lesion.

   (a) FCD Type IIIa - This type is associated with hippocampal sclerosis and is characterized by cortical dyslamination and hypertrophic neurons located outside of layer 5. Additional subtypes of Type IIIa exist, each linked to the primary disease causing the malformations.

   (b) FCD Type IIIb - Associated with tumors, this condition presents with cortical dyslamination, hypoplasia, and hypertrophic neurons located adjacent to the neoplasm.

The mechanism by which neoplasms induce FCDs and, in some cases, subsequent seizures remains unknown.

(c) FCD Type IIIc - Associated with vascular malformations, this condition also features cortical dyslamination and hypertrophic neurons adjacent to the vascular malformation. These FCDs are typically linked to abnormal sulcation and a large primary vein responsible for draining them.

(d) FCD Type IIId - Associated with any major lesion acquired during early life, this condition presents with similar cortical dyslaminations and hypertrophic neurons of the neocortex. It is acquired through early-life complications such as traumatic brain injuries, glial scarring, and various inflammatory and infectious diseases.

Given this complexity surrounding FCDs, and their direct contribution to seizures, it follows that their correct identification in a given MRI scan, specially before surgery, is of the utmost importance to improve clinical success, as proven, independently by these two articles(12)(37).

2.5 Neuroimaging in Epilepsy

The introduction of imaging technology in epilepsy revolutionized the field, allowing for a detailed determination of disease etiology and subsequent improved clinical decisions. Given the importance of explaining the origin of the seizures in each patient, utilizing MRI and other imaging methods like Computerized Tomography (CT) and Positron Emission Tomography (PET) becomes essential. CT is a valid option for urgent situations, where excluding certain medical conditions within a strict time constraint is essential to properly deal with the clinical situation. For example, if there is suspicion of brain hemorrhage, lesions with calcifications, or large tumors, CT proves to be a more readily available, cheaper, and quicker methodology than MRI(38). Regardless, MRI has been shown to identify brain lesions characteristic of epilepsy in 8%-12% of patients with healthy CT scans(39). PET is typically performed alongside MRI in refractory focal epilepsy patients. It aids in the localization of the lesion, approximating the theoretical epileptogenic zone with the real region to be resected. PET scans are typically co-registered with MRI, meaning they are overlapped with a consistent anatomical template, thus allowing for a more nuanced clinical interpretation of the brain lesions, with a higher detection rate of FCDs(40).

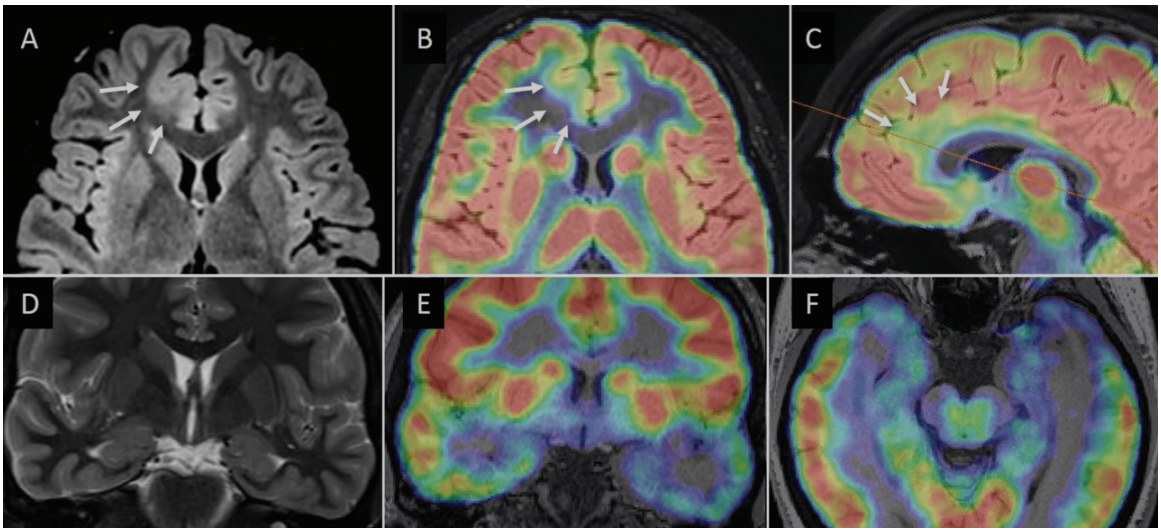

Figure 2.2: Co-registration of MRI and PET. Localization of an FCD is showcased by the arrows in different anatomical views. Adapted from (41).

MRI, specifically for refractory focal epilepsy patients, is the most important and typically the determinant factor in planning the surgical procedure. As mentioned in (42), every epilepsy patient should have an MRI performed, except for very specific cases. The usual MRI protocol for epilepsy includes obtaining T1-weighted 3D and fluid-attenuated inversion recovery (FLAIR) scans. Each sequence offers different imaging benefits depending on the specific epilepsy syndrome and structural cause. In the case of FCDs, their visibility in the different scans is usually dependant on their subtype. For FCDs type I, a typical finding is the dissolution of the grey-white matter boundary, which may appear as a very bright (hyperintense) spot on FLAIR, sometimes also present in T1(10).

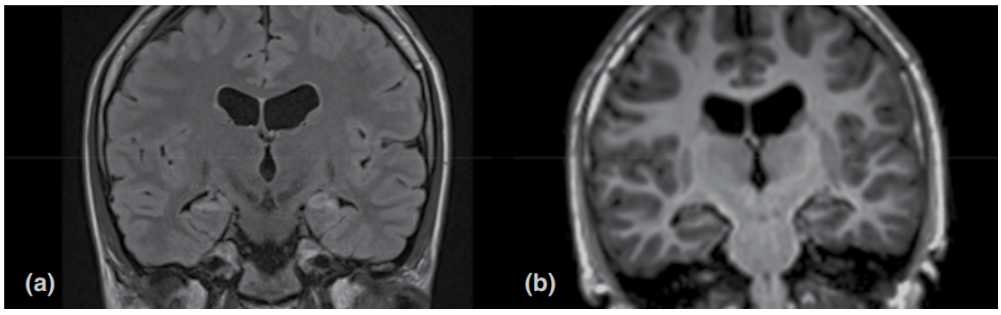

Figure 2.3: FLAIR (a) and T1 (b) with hyperintensity displayed in both mesial temporal lobes, characteristic of mesial temporal sclerosis(43), a condition that induces seizures. Adapted from (44).

For FCDs type IIA, given their characteristic dysmorphic neurons, but without the relatively visible balloon cells, the signal perceived in MRI is usually very discreet. FCDs of type IIB are characterized by the presence of balloon cells that contribute to a thickening of the cortex, and an abnormal cortical gyration. Both structural abnormalities are reflected as hyperintense FLAIR signals, typically more intense than in FCDs of type I(10).

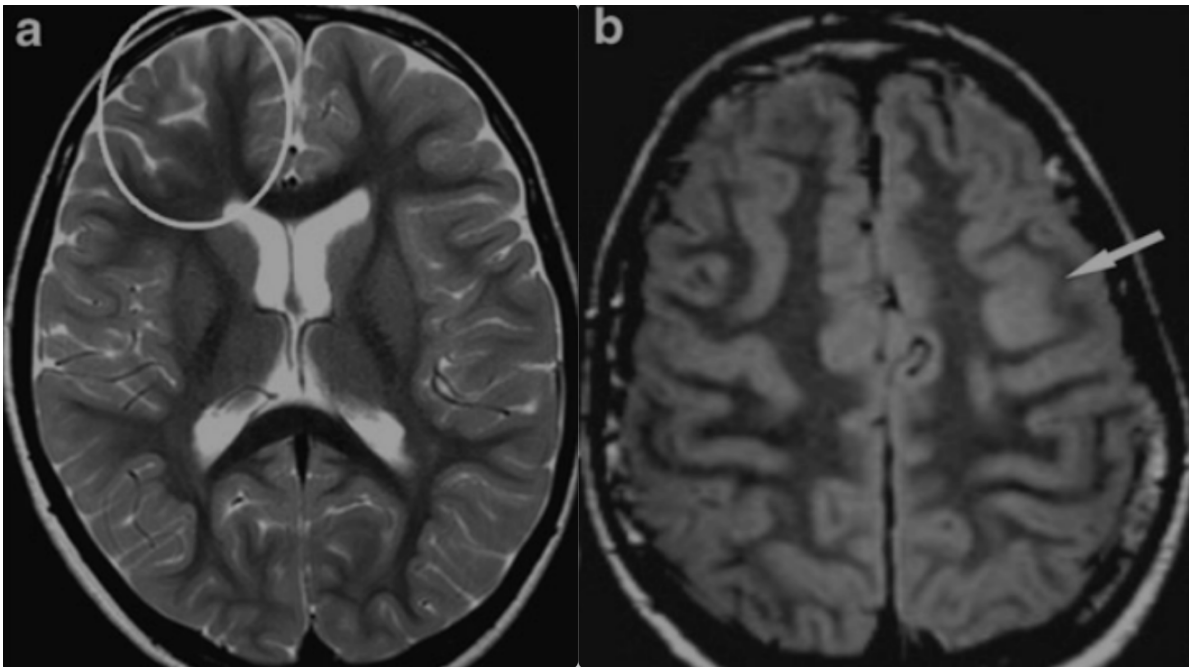

Figure 2.4: FCD type IIa (a) and FCD type IIb (b) in T2 and FLAIR scans respectively. Adapted from (45).

Chapter 3

Computer-assisted Detection of FCDs

FCDs are one of the most common causes of refractory focal epilepsy. Their correct clinical assessment is paramount in planning a surgical intervention that aims at reducing the experienced seizures to a manageable frequency and intensity. Neuroimaging techniques, especially MRI, are used to delineate the FCD's region and determine the epileptogenic zone, which corresponds to the theoretical minimum tissue area considered for resection. Traditional visual inspection of MRI has limitations, as it can be time-consuming, prone to inter-observer variability, and has a high error rate, determined by comparing pre-surgical visually identified FCDs with post-surgical histopathological studies, alongside observing if the symptoms are lessened or not(13). This reduction in the seizure occurrence is directly correlated with the amount of removed tissue considered to be an FCD. An incomplete resection increases the likelihood of the patient experiencing post-operative seizures(46)(47) which may only be alleviated by a secondary surgical intervention. All of these factors contributed to the necessity of developing computer-assisted methods that aimed at aiding clinicians in identifying FCDs with greater accuracy and consistency.

3.1 Brain Morphometry

The first group of methods used to aid in the detection of FCDs falls under the category of Brain Morphometry. Although this technique was initially developed around 1970(48), it was in the late 1990s and early 2000s, due to the improvement in image quality obtained via MRIs and advances in the necessary computational tools, that brain morphometry expanded and became a very sought after technique to further analyze medical imaging scans(49). This analysis focuses

on measuring the size, volume, and shape of different brain structures and their tissue types. Brain morphometry enables the shift from qualitative analysis of medical imaging scans, to a quantitative assessment of brain anatomy allowing the identification of structural abnormalities associated with neurological conditions such as epilepsy. Given the structural nature of FCDs, brain morphometry evidently becomes an essential tool to be used when dealing with refractory focal epilepsy.

3.1.1 Voxel-based Morphometry

One of the most commonly used brain morphometry techniques is Voxel-based Morphometry (VBM)(50). The term "voxel," derived from "volumetric pixel," refers to the individual element that makes up volumetric medical imaging scans and whose intensity value is represented by its brightness on the image. In VBM, a voxel-wise comparison is performed between 2 groups of images, typically T1-weighted MRI scans, calculating their differences in grey matter concentration. This statistical calculation is performed throughout the whole brain, without any pre-selection of preferred regions, allowing for a homogeneous, bias-free analysis, that helps reveal the structural nature of diseases like Alzheimer's(51), schizophrenia(52), attention-deficit/hyperactivity disorder(53) and of course epilepsy(54).

3.1.1.1 Processing steps

VBM's processing includes several steps that can change depending on the software used and the purpose of its utilization. Most VBM pipelines are divided into a preprocessing stage that includes skull stripping and signal nonuniformity correction and a main processing stage that includes tissue segmentation, spatial normalization, image smoothing, and statistical analysis.

1. Skull Stripping(55) - Also commonly referred to as Brain extraction, this step aims to remove any image data that pertains to the skull, the scalp, the eyes, and other non-brain tissue. Subsequent processing steps, including the final statistical analysis, are performed on images that only portray the cortex and cerebellum which are the relevant anatomical structures for most VBM studies. Removing unnecessary components also decreases the likelihood of artifacts arising during the pipeline and increases the signal-to-noise ratio.

This step is performed in many different ways but it typically involves morphological techniques alongside edge detection to delineate the regions considered for removal(56). With the increased interest in using Deep Learning in the medical world, several methods have been implemented to perform skull stripping with admirable results(57)(58).

2. Signal Nonuniformity Correction(59) - This step attempts to address the inherent inhomogeneities in the MRI machine's magnetic field specifically the B1 field. The B1 field refers to the radiofrequency magnetic field used to excite the protons in the body during MRI scans. It is perpendicular to the main magnetic field, known as the B0 field, which is a static and uniform field that aligns the protons' magnetic moments. It also serves to alleviate the impact of the noise introduced by analog-to-digital converters, gradient-driven eddy currents, radio frequency penetrations and the hardware properties of individual scanners(60) to obtain a more statistically coherent image, with an even intensity representation of the brain tissue, better suited for comparisons with others from different setups. This is achieved by estimating the contribution of each of the aforementioned possible noise sources, combining them in a mask, and subtracting it from the original image. To calculate this mask several methods exist but they typically revolve around using a Finite Gaussian Mixture (FGM) model(61) or a Hidden Markov Random Field (HMRF) model(62) and combining them with a deformable template that represents the a priori tissue type (grey matter, white matter and cerebrospinal fluid) probability across the whole image. By using FGM we assume that the intensity distribution of each tissue type can be modeled as a Gaussian distribution, allowing for the iterative fitting of the deformable template to the original image thus estimating the parameters that best describe the noise and the true signal. A second approach is to consider each intensity at every voxel as an independent variable and generalize the typical signal nonuniformity effect on the image as a blur, that reduces the representation of the high-intensity sections on the image. Given this, an iterative process begins, that aims at sharpening the blurred sections and estimating the noise distribution(59)(63).

3. Tissue Segmentation - In this step, the brain tissue is classified into different components, such as gray matter, white matter, and cerebrospinal fluid. Some segmentation algorithms

rely on a priori tissue distribution maps to assess the probability for each voxel of belonging to a given tissue class. From this, by fitting the image to a known standard anatomical space and choosing intensity threshold values for each tissue class the classification of each voxel is performed(61). Other algorithms, that do not rely on a priori tissue information, use spatial cohesion as their main focus. Through the use of an HMRF model, the label of neighboring voxels is also taken into account, allowing for a more informed classification and removing the need to fit the image to a standard anatomical space(62). Tissue segmentation is crucial, as it allows for the quantification of gray matter density, which is the primary focus of most statistical analyses characteristic of VBM.

4. Spatial Normalization - Spatial Normalization as a processing step in VBM is used to transform individual brain images into a common stereotactic space and align them with a standardized brain atlas such as the Montreal Neurological Institute (MNI) template(64) or with a study-specific template, created with a group of images relevant to the analysis being performed(65). It essentially scales differences between the different MRI scans, their sizes and shapes, important to normalize so that each voxel has a similar anatomical location across all images. By utilizing linear and nonlinear transformations, spatial normalization makes it possible to compare the subject's brain structures with the template thereby enhancing the subsequent voxel-wise comparisons and statistical analyses amongst groups of subjects. This ensures consistent structural differences and avoids mistaking inter-structural variations for true inter-subject differences, reducing errors associated with morphometric studies.

5. Smoothing - During this step, a Gaussian smoothing kernel is applied to the brain images, blurring the data and enhancing the signal-to-noise ratio. This step spreads the intensity values across neighboring voxels, compensating for anatomical variability and minor misalignments that may occur during spatial normalization. By increasing spatial correlation between voxels, image smoothing makes it easier to detect significant regional differences in gray matter concentration. The relevant image features that could uncover structural abnormalities in the brain remain prominent after this step, whilst the surrounding artifacts that contribute to a decrease in signal-to-noise ratio are dispersed amongst neighboring data. Given this, a big emphasis is placed on which size of the Gaussian kernel to use, as shown

in (66) and (67). If the chosen kernel size is appropriate for the anatomical characteristics of the structure being studied, pathological or not, then this process not only improves the statistical power of subsequent analyses but also ensures that the data remains robust against minor variations.

6. Statistical analysis - After the final processing step of smoothing the image, the relevant gray matter density analysis is ready to be performed. Most VBM studies conducted, calculate this voxel-wise comparison between 2 groups of subjects, typically healthy and patient, and also investigate possible correlations between gray matter density and certain variables of interest such as age or cognitive score. Commonly used statistical tests include t-tests(68), analysis of variance (ANOVA)(69) and regression analyses(70). Given the inevitable confounding variables that exist between the study groups, the general linear model (GLM) is used to control for these confounders and ensure that observed differences in gray matter density are attributable to the variable(s) of interest and not external factors. An important aspect of the GLM is its flexibility concerning complex relationships that may exist in neuroimaging data, by allowing to model gray matter density in each voxel as a function of other explanatory variables. Once the model has been defined, it will produce statistical maps showing significant differences between voxels or significant correlations among them. Nevertheless, due to their large number, multiple comparison correction techniques such as family-wise error (FWE)(71) correction and false discovery rate (FDR)(67) correction are employed to curb false positives and guarantee the stability of findings. Additionally, as demonstrated below, standard brain templates can be used to graphically represent these results to provide anatomical context for understanding structural brain changes occurring in various pathological conditions.

3.1.1.2 VBM for FCD detection

A major advantage that VBM provides is the ability to do voxel-wise comparisons across the whole brain. This analysis enables the identification of areas with significant differences in gray matter which may be suggestive of FCDs, unlike traditional methods which depend on visual inspection only. Additionally, unlike other approaches that look at brain regions individually, this method can help identify multiple sites at once, which could further aid in surgery planning.

Because of this step-by-step computation, the inter-observer variability is also reduced leading to more consistent and reproducible results, essential to further understand the structural correlates of brain diseases.

Many studies have shown how effective VBM can be when it comes to the detection of FCDs. For example, as shown in (72), VBM was used to analyze MRIs of focal epilepsy patients who continued experiencing seizures even after surgical intervention was performed. A group of 11 patients with visually detected FCDs were compared to a group of 96 healthy controls with age being considered as a confounding variable in the chosen statistical test. The results reveal an excess amount of gray matter in the FCD population in 10 out of the 11 patients, with 7 of them displaying an excess larger than the originally considered FCD region. Assessing the presence and location of FCDs with VBM pre-surgically could have improved the clinical outcome of the patients. As demonstrated in (73), where 150 patients candidate for surgery and considered to be MRI negative (meaning that no lesion was visually detected), had their pre-surgical imaging scans analyzed by VBM. Patients with a positive FCD finding with VBM also experienced the best post-surgical reduction in seizures, proving the utility of VBM in more accurately delineating the epileptogenic zone considered for resection. The clinical outcome improves when there is a minimal discrepancy between the resected area and the area identified by VBM. Another study(74), conducted in 2024, proposed to investigate the structural brain correlates for cognitive impairment in children with FCDs. This study involved 25 pediatric patients with pharmacoresistant epilepsy due to confirmed FCD and 25 healthy controls.

The cognitive evaluations found Wechsler Intelligence Scale for Children, Fourth Edition (WISC-IV) indices to be significantly lower in the FCD group than in healthy controls. In the left cerebellum, bilateral thalamus, and right precuneus, VBM detected increased grey matter volume with decreased grey matter volume in the bilateral medial frontal gyrus along with the left inferior temporal gyrus. These structural abnormalities have associations with cognitive impairments that underscore disruptions of neurodevelopment among children who experience early-onset seizures.

These findings also demonstrate VBM's ability to identify not only FCDs but also regions where gray matter increases or decreases across the whole brain. This understanding improves diagnosis accuracy and helps us better understand epilepsy-related disturbances during neurodevelopment.

However, there are limitations and concerns about VBM. One major issue is the image normalization accuracy. VBM relies on aligning brain images precisely with a standard template which

may be difficult for patients with epilepsy due to lesions or other structural abnormalities that can cause misalignment thereby leading to incorrect evaluations of changes in brain morphology(75). Another limitation involves sensitivity to pre-processing choices, various factors like MRI sequence type used, image processing parameters set or statistical methods applied could affect results obtained from VBM as such making it hard to standardize procedures across different studies and thus causing inconsistent findings(76).

In addition to mainly providing volumetric information on brain structures, VBm does not account for functional aspects related to epileptic activity. While VBM is important for understanding structural changes associated with epilepsy, it does not fully capture the functional dynamics of the brain. Combining VBM with functional imaging techniques such as fMRI or PET scans is essential to address this limitation. These methods can provide a more comprehensive understanding by monitoring brain functions alongside structural changes.

Therefore, it is important to understand that VBM is an effective method of measuring brain structure, particularly in studying epilepsy, however, other techniques need to be applied alongside it not to limit the scope and accuracy of analysis.

3.1.2 Surface-based Morphometry

Another commonly used neuroimaging analysis method is Surface-based Morphometry (SBM). While VBM focuses on analyzing gray matter volume throughout the brain, SBM facilitates detailed analysis of cortical surfaces, allowing the study of brain features such as cortical thickness, surface area, and gyrification patterns. SBM can be used to aid in the clinical process of many diseases such as tinnitus(77), Alzheimer's(78), Huntington(79), epilepsy(80)(81) and even to analyze differences in the brain of carbon monoxide patients(82). SBM shares some similarities with VBM, namely their processing steps of skull stripping, signal nonuniformity correction, tissue segmentation, spatial normalization, smoothing, and statistical analysis, although some of these are performed in slightly different ways:

1. Tissue Segmentation - In SBM, the image is also segmented into gray matter, white matter, and cerebrospinal fluid but the method to achieve this is different. From the image, the white matter and pial surfaces are created(83) with their borders being determined via an analysis of voxel intensity. The first surface splits the brain into its white matter and grey matter

regions while the second specifies the separation between grey matter and cerebrospinal fluid. Then, the white matter is divided between the two hemispheres of the cerebral cortex and the surface of each hemisphere is tessellated. During tessellation, each voxel on the border is split into a square with two triangles thereby separating gray substance from white matter. After smoothing these surfaces made of tessellated white matter, pial surfaces are determined by expanding them. The shortest distance between each white matter vertex and the pial surface determines cortical thickness. Additionally, the cortical area around each vertex is calculated by taking the average of all the triangle areas that include that vertex. Gray matter volume is then obtained by multiplying this area by the cortical thickness. Next, the whole brain gyrification index is defined as the total pial surface divided by the total perimeter of the brain which can be acquired through shape-smoothing. Local gyrification index calculates folding degree at specific regions on cortical surfaces offering crucial information about cortical morphology.

2. Spatial Normalization - Given this focus on cortical morphology, a template needs to be standardized and used as a coordinate system for the different brain structures and regions studied. The white matter surface extracted during tissue segmentation is inflated into a sphere transferring the 2D representation of the white matter geometry into 3D(84). The registration to a common stereotaxic space is then performed on the inflated surface, through a non-linear, iterative folding that aligns the cortical patterns of the image with the ones in the template.

3. Statistical analysis - Performed similarly to VBM but with the added metrics generated by the SBM processing. These include cortical thickness, area, volume, gyrification patterns, and more. This analysis is performed vertex by vertex, relying on statistical tests and the GLM to study relationships between relevant study metrics.

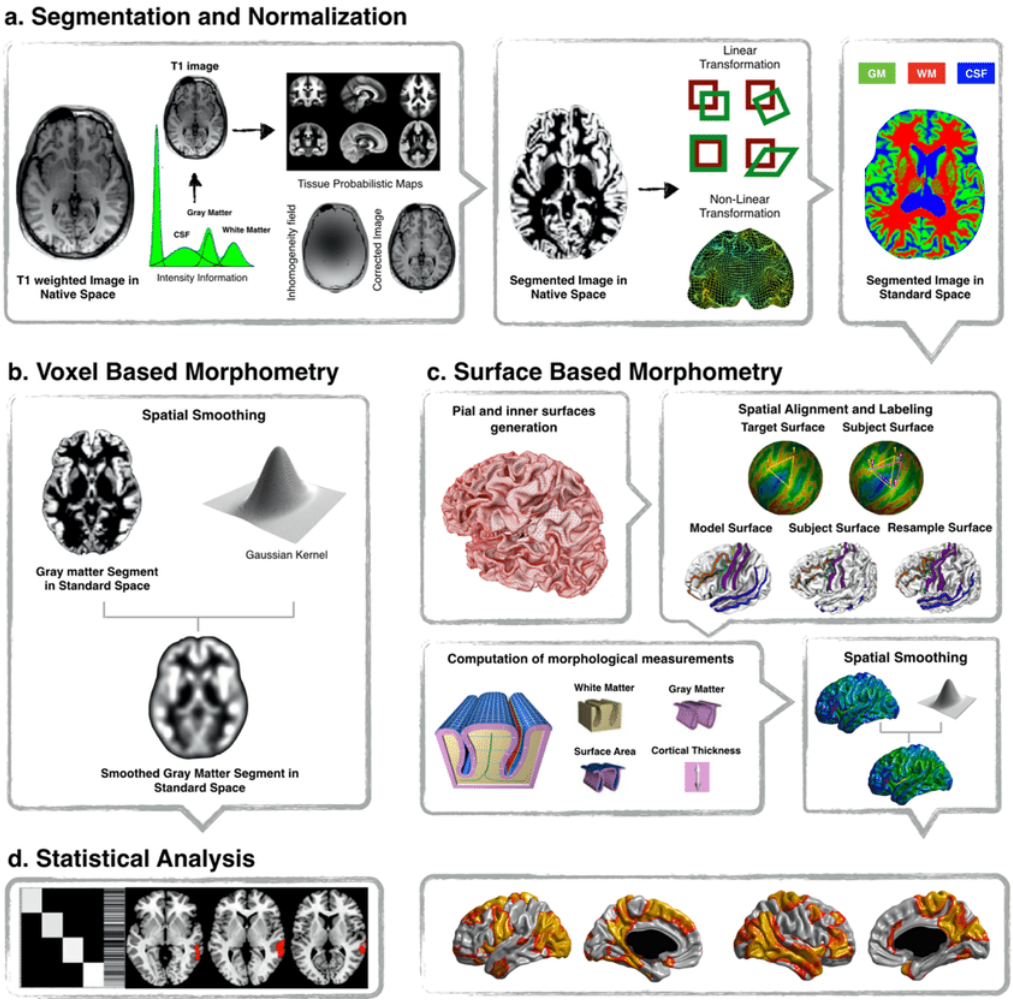

Figure 3.1: Pipeline detailing typical VBM and SBM processing. Adapted from (85)

3.1.2.1 SBM for FCD detection

Given FCD's propensity to increase cortical thickness(86), to affect surface gyral anatomy, and to blur the gray-white matter barrier(87), the additional surface features that SBM provides aid in the identification and delineation of FCDs in MRI scans. According to this definition, SBM can detect slight cortical defects that are not visible through conventional imaging methods by giving precise measurements of cortical thickness, surface area, and gyrification. These intricate features of the surface provide a better understanding of the shape of the cortex which makes it easier to identify parts with abnormal development, which can be associated with FCDs, more accurately. Abnormal gyrification often seen among patients suffering from FCD can be quantitatively assessed using this method thereby providing a clearer picture about how much or what type of malformation has taken place in different parts across the brain surface. Unfortunately,

given the heavy data processing associated with brain morphometry methods, and the inherent high variability of FCD lesions, SBM's detection accuracy can be limited, especially when used on its own. A popular method of improving this is using the features extracted using SBM as inputs for ML models(88). ML can enhance SBM by automating the analysis of these complex features, reducing subjective biases, and providing more consistent and accurate diagnoses. This integration not only improves diagnostic precision but also expedites the process, making it more efficient and less reliant on individual radiologist expertise and time restrictions.

3.2 Machine Learning based methods

ML is a set of methods that leverage statistics and large amounts of data to learn patterns relevant to us(89). ML has been employed in several fields, with medicine being a very popular one(90). Specifically for epilepsy, ML has brought several improvements, including automatic seizure detection in electroencephalogram recordings(91), diagnosing Juvenile Myoclonic Epilepsy(92) and of course detecting FCD in MRI images(93). The usability and performance of a given ML model are highly dependent on the input it receives, with several different approaches typically being considered for the same use case. In FCD detection, a typical divide happens between the methods that directly use MRI scans, in the form of voxel data, as inputs for Deep Learning (DL) (a subset of ML) models, typically Convolutional Neural Networks (CNNs) and the methods that employ some pre-processing to extract relevant features from the images and use them as inputs.

3.2.1 Convolutional Neural Networks for FCD detection

DL models such as CNNs can perform feature extraction automatically, thus allowing for raw image data input. This potentiality paves the way for more elaborate analysis of neuroimaging data, especially in the detection of FCDs. Unlike conventional methods that depend much on manual feature extraction and professional interpretation, CNNs can learn complex patterns and structural abnormalities directly from MRI scans.

Convolutional layers, pooling layers, and fully connected layers make up a typical CNN. Each layer has its specific role in processing and analyzing images. During convolutional layer operations, filters are applied to input images creating feature maps that indicate important patterns like edges, textures, and shapes. Pooling layers then reduce the dimensionality of these feature maps

while retaining the most significant information thus reducing computational load. Finally, fully connected layers interpret these features to determine the presence of FCDs.

Such a hierarchical approach allows CNNs to capture both low-level details and high-level structures within brain images effectively. For FCD detection this implies that subtle cortical abnormalities which might be missed by traditional approaches, either visual inspection or brain morphometry, can be identified more accurately.

CNNs can be trained using large datasets whereby their performance keeps improving with increased availability of data. This continuous ability to learn is very useful, especially in the medical field where there is a constant generation of new data which may lead to stronger models that can be generalized more easily.

Several studies have been conducted applying CNNs to FCD detection such as in (94), where a relatively simple CNN model received cortical patches extracted from axial slices of MRI brain scans pertaining to 10 FCD patients and 20 healthy controls. Although the dataset size is limited, the results are still relevant with a 90% sensitivity (ability to correctly identify true positives) and 85% specificity (ability to correctly identify true negatives). Another study, decided to focus on the applicability of their model to various clinical contexts, creating a dataset from multiple epilepsy centers and hospitals(95). A cohort of 149 epilepsy patients, 51% of which were considered MRI negative, was created from 9 different centers. Similar to the aforementioned paper, patches were extracted from the MRI volumes and used as input to the CNN model. An overall sensitivity of 93% was achieved, meaning that 137 out of the 148 FCDs were correctly detected. A dedicated independent cohort was created that only featured images that were not used in the training of the model in order to evaluate external performance, perhaps when applied to a new center or hospital. In this cohort, a sensitivity of 83% was achieved, confirming the robustness and usefulness of this proposed method. Unfortunately, using CNNs to automatically detect FCDs has a very considerable limitation. Known as the "black-box problem" in the DL field, these models fail to explain the reasoning behind the decisions they make, limiting the interpreter's understanding of the patterns being learned from the data provided. This lack of transparency can hinder the acceptance and trust of these models in clinical settings, as healthcare professionals often require clear justifications for diagnostic decisions to ensure patient safety and treatment efficacy. Furthermore, the black-box nature of CNNs can make it challenging to identify and correct errors or biases within the model, potentially affecting the reliability of the results across different patient

populations and imaging conditions.

3.2.2 Combined ML and feature extractor methods

Combining feature extraction techniques with traditional ML models offers a compelling solution to the challenges posed by the black-box nature of DL models. ML models combined with feature extractors such as VBM and SBM provide a more interpretable approach, allowing clinicians to comprehend and trust the diagnostic process.

Traditional ML models, such as support vector machines (SVM), decision trees, and logistic regression, rely on explicitly defined features extracted from the data, which allows clinicians to trace back the decision-making process and understand which specific characteristics contributed to a diagnosis. This transparency is crucial in a medical context, where understanding the basis for a diagnosis can significantly impact treatment decisions and patient outcomes.

The combined approach of feature extraction and ML enhances both interpretability and performance. By leveraging the strengths of VBM and SBM, this methodology captures complex patterns in neuroimaging data that might be missed by a singular approach. For instance, features derived from VBM can highlight volumetric abnormalities, while SBM features provide detailed surface measurements. When these complementary features are fed into ML models, the result is a significant improvement in the detection and localization of FCD lesions.

Several studies have demonstrated the effectiveness of this combined approach. For example, (96) used SBM-derived features in conjunction with a simple ML model of logistic regression to detect FCD in MRI-negative patients, achieving a 86% detection rate. Another study, employed VBM to generate gray matter concentration maps, which were then analyzed using SVM classifiers to identify FCD lesions, achieving a detection rate of 98%(97).

3.3 Overview of available software

This chapter provides an overview of the major software available for voxel-based morphometry (VBM), surface-based morphometry (SBM), and other open-source methods for detecting FCDs.

3.3.1 Voxel-based Morphometry

1. SPM (Statistical Parametric Mapping)(98) - SPM is a widely-used software package for the analysis of brain imaging data sequences. It implements a standard approach to VBM, enabling the preprocessing, normalization, and statistical analysis of structural MRI data.

   Key Features: SPM offers tools for spatial normalization, tissue segmentation, and smoothing. It also provides a flexible framework for statistical analysis and simple visualization of results.

   Applications: SPM is extensively used in research for studying structural brain changes associated with various neurological and psychiatric conditions, including focal epilepsy.

   Advantages: Robust set of tools, widely used and supported, with a very useful statistical framework.

   Disadvantages: Can be complex to use for beginners, requires significant preprocessing, limited visualization capabilities compared to some other tools.

2. CAT (Computational Anatomy Toolbox)(99) - CAT is an extension of SPM that focuses on computational anatomy and morphometry.

   Key Features: It includes advanced tools for tissue segmentation, cortical thickness estimation, and surface reconstruction. CAT also offers improved normalization procedures and varied statistical tests.

   Applications: CAT enhances the capabilities of SPM for more detailed morphometric analyses, making it a valuable tool for FCD detection.

   Advantages: Enhanced features over standard SPM, more detailed and accurate morphometric analysis, robust statistical tools.

   Disadvantages: Still requires familiarity with SPM, may have a steep learning curve, computationally intensive.

3. ANTs (Advanced Normalization Tools)(100) - ANTs is an open-source software suite for image registration and segmentation, often used in VBM.

Key Features: ANTs offers state-of-the-art registration algorithms, cortical thickness measurement, and tissue segmentation tools. It is highly customizable and integrates well with other software packages.

Applications: ANTs is used in conjunction with other tools for detailed morphometric analyses and the detection of cortical abnormalities.

Advantages: High accuracy in image registration and normalization, flexible and customizable, integrates with other tools.

Disadvantages: Can be complex to set up and use, may require significant computational resources, less user-friendly than some alternatives.

3.3.2 Surface-based Morphometry

1. BrainVISA(101) - BrainVISA is a software platform for neuroimaging research that supports a wide range of morphometric analyses.

   Key Features: It includes tools for cortical surface reconstruction, sulcal pattern analysis, and cortical thickness measurement. BrainVISA also supports data integration and visualization.

   Applications: BrainVISA is used for detailed morphometric studies, including the analysis of cortical dysplasias and other brain malformations.

   Advantages: Versatile and comprehensive, good integration with other tools, strong visualization capabilities.

   Disadvantages: Can be complex to use and set up and requires substantial computational resources.

2. CIVET(102) - CIVET is an automated pipeline for comprehensive brain imaging analysis developed by the Montreal Neurological Institute.

   Key Features: CIVET includes tools for cortical thickness measurement, surface extraction, and volumetric analysis. It is designed for robust and reproducible morphometric studies.

   Applications: CIVET is used in large-scale brain imaging studies and provides detailed morphometric data that can be used for detecting cortical abnormalities like FCD.

Advantages: High reproducibility, robust pipeline for large datasets, detailed cortical measurements.

Disadvantages: Requires significant computational resources, may be less user-friendly, steep learning curve.

3. FreeSurfer(103) - FreeSurfer is a comprehensive software suite developed by the Martinos Center for Biomedical Imaging at Massachusetts General Hospital. It is designed for the processing and analysis of human brain MRI images. FreeSurfer is widely used and particularly renowned for its capabilities in SBM.

   Key Features: FreeSurfer provides automated tools for the reconstruction of the brain's cortical surface from structural MRI data. It includes detailed measurements of cortical thickness, surface area, and gyrification index. FreeSurfer also offers robust registration and parcellation of brain regions based on anatomical landmarks. Additionally, it performs subcortical segmentation to identify and measure structures such as the hippocampus, amygdala, and basal ganglia.

   Applications: FreeSurfer is widely used in neuroimaging research for studying brain morphology and identifying abnormalities such as FCDs. Its detailed surface-based analysis allows researchers and clinicians to detect subtle cortical changes and abnormalities with high precision. It is particularly valuable for longitudinal studies, allowing for consistent measurements over time.

   Advantages: FreeSurfer's automated pipeline provides accurate and reproducible results. Its comprehensive set of tools for morphometric analysis makes it a preferred choice for many researchers in the field. The software is well-documented and supported by an active user community, which facilitates troubleshooting and the sharing of best practices.

   Disadvantages: FreeSurfer can be time-consuming to process large datasets, as it requires significant computational resources. New users may face a steep learning curve due to the complexity of its features and the need for extensive preprocessing. However, the investment in learning FreeSurfer is often justified by the high-quality results it produces.

3.3.3 Open-source ML FCD detection

Although there are some open-source methods that offer a fully functional, albeit non-trivial to deploy clinically, FCD detection method, such as (95) and (104), they typically do not attempt to alleviate the complications that arise from the aforementioned black-box problem, limiting their clinical usefulness. A third method, created by the researchers at the Multi-centre Epilepsy Lesion Detection (MELD) project, encompasses the efficacy and explainability of traditional ML with the power yearned from the clinically relevant brain surface features extracted using SBM, more specifically FreeSurfer. It also produces clinically relevant outputs that not only display the algorithm's prediction but also a PDF file outlining the reasoning for the decision. To accomplish this, the following methodology was followed(105):

1. Participant Demographics

   Data was collected from a diverse group of participants, including both patients with epilepsy and control subjects without epilepsy. Key demographic information included age at preoperative scan, sex, age of epilepsy onset, duration of epilepsy, MRI-negative status, histopathological diagnosis, seizure freedom, and follow-up time for operated patients.

2. Data collection and pre-processing

   MRI scans, specifically 3D T1-weighted and FLAIR images (when available), were collected from 22 participating centers using Siemens, GE, and Philips MRI scanners at either 1.5 or 3 T field strengths. Cortical surfaces were reconstructed using FreeSurfer software, which the sites processed on either Linux or Mac operating systems using FreeSurfer versions 5.3 or 6.

3. Lesion Masking

   FCD lesions were delineated on T1-weighted MRI scans at each site following a standardized lesion masking protocol. For radiologically diagnosed FCD patients, volumetric lesion masks were created using preoperative T1 and 3D FLAIR scans. In MRI-negative patients confirmed by histopathology, postoperative scans were used to identify the FCD location on preoperative images, followed by volumetric lesion mask creation. These masks were reviewed and created by a neuroradiologist, neurologist, or experienced epilepsy researcher

at each site, and were further refined using a dilation–erosion algorithm and registered to a symmetric template surface.

4. Morphological and Intensity Features

   Several measures were calculated per vertex across the cortical surface in all participants:

   (a) Cortical Thickness - The mean minimum distance between each vertex on the pial and white matter surfaces.

   (b) Grey–White Contrast - The ratio of T1 grey matter signal intensity to white matter signal intensity.

   (c) Mean Curvature - Calculated at the grey–white matter boundary.

   (d) Sulcal Depth - Calculated using the dot product of the movement vector of the cortical surface during inflation.

   (e) Intrinsic Curvature - Calculated as the dot product of the principal curvatures.

   When FLAIR data was available, multiple cortical depths were analyzed, retrieving the signal intensity of each.

5. Centralized Quality Control and Data Harmonization

   To ensure high-quality data, automated quality control identified subjects with extreme structural and intensity values across multiple cortical areas, likely due to imaging artifacts. Features were harmonized using ComBat(106) to control for non-biological variance while retaining biological covariates such as age, sex, and disease status.

6. Three-stage feature normalization

   The normalization procedure was conducted in three stages:

   (a) Intrasubject Z-scoring - Normalized features to account for age and sex-related changes.

   (b) Interhemispheric Asymmetry - Created by subtracting right hemisphere vertex values from left hemisphere values to leverage normal symmetry and highlight FCDs.

   (c) Per-vertex Normalization by Controls - Adjusted features by comparing them to healthy control values to account for normal interregional variability.

7. Neural Network Classifier and Performance Evaluation The study trained a neural network classifier using the extracted surface-based morphological features to detect FCD lesions. The classifier's performance was evaluated using multiple metrics, including sensitivity, specificity, and cluster detection rates. Logistic regression models assessed the influence of demographic and clinical factors on lesion detection, while integrated gradients saliency(107) helped understand which features influenced network predictions.

From this methodology, a fully functional FCD detection algorithm emerges with a per-patient output that displays information regarding the different considered FCD clusters as well as information regarding what led to the algorithm's decision.

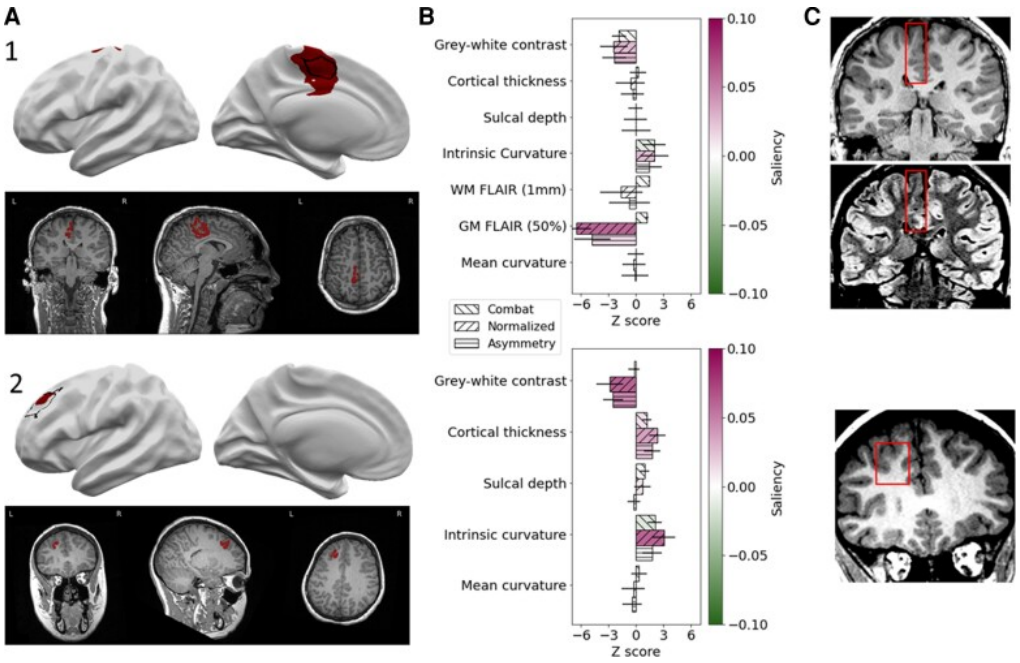

Figure 3.2: Example of individual patient output. Adapted from (105)

Although MELD's implementation focused on generating clinically relevant outputs, incorporating it into the clinical workflow still has some complications. The reliance on FreeSurfer forces the use of Mac OS X or Linux operating systems, the installation of both FreeSurfer and MELD is not trivial, some knowledge of terminal commands, Python environments, and executing scripts, and the file management throughout the whole process is not straightforward enough for clinicians that have very high time constraints.

Chapter 4

Methodology

Considering the goal of providing an easy solution to integrate a relevant automatic FCD detection method into the clinical workflow, the focus was placed on verifying MELD's usability for HSA's use case and encapsulating it into a functional GUI. Exemplary MRI data with FCD regions delineated was provided and processed to test the usability of the developed implementation.

4.1 Data Collection and pre-processing

The data provided consisted of 7 pairs of T1 and FLAIR MRI scans, each pertaining to a refractory focal epilepsy patient with confirmed FCDs. All the data provided followed appropriate anonymization methods and received the necessary clearance from the relevant ethics committee. Image acquisition was performed on an MRI scanner Achieva 3.0T TX Software release 5.4.1.1 (Phillips Medical Systems). All the images were acquired in the Neuroradiology Department at Unidade Local de Saude Santo António. All data were acquired using a 32-channel phased-array head coil. T1-weighted images consisted in a 3D T1-TFE sequence with the following parameters: TE = 2.948 ms, TR= 6.557 ms and flip angle of 8°. The images had a voxel resolution of $1 \times 1 \times 1$ mm 3 , square FOV of 240 mm with a reconstructed matrix size of 512×512. The 3D T1-TFE sequence is a fast 3D gradient echo pulse. T2-weighted images were based on a 3D FLAIR sequence with the following parameters: TE = 340 ms, TI = 1650 ms, TR = 4800 ms and a flip angle of 90°. The acquisition voxel resolution of these images is $1.11 \times 1.11 \times 1.12$ mm (reconstructed to $0.88 \times 0.88 \times 0.56$ mm 3) using a square FOV of 240 mm. All acquired images were reviewed on the Picture Archiving and Communication Systems (PACS) system (Sectra

IDS7, Version 24.2.6.5829 Sectra AB, Linköping, Sweden) and annotations with segmentation of the lesion (FCD) were performed directly at the Sectra viewer with the ROI area tool. Manual segmentation was performed by a 7-years experienced neuroradiologist based on T2-FLAIR hyperintensity and loss of sharp cortex-subcortical white matter transition. The annotated images were then anonymized and exported from the visualizer in DICOM format.

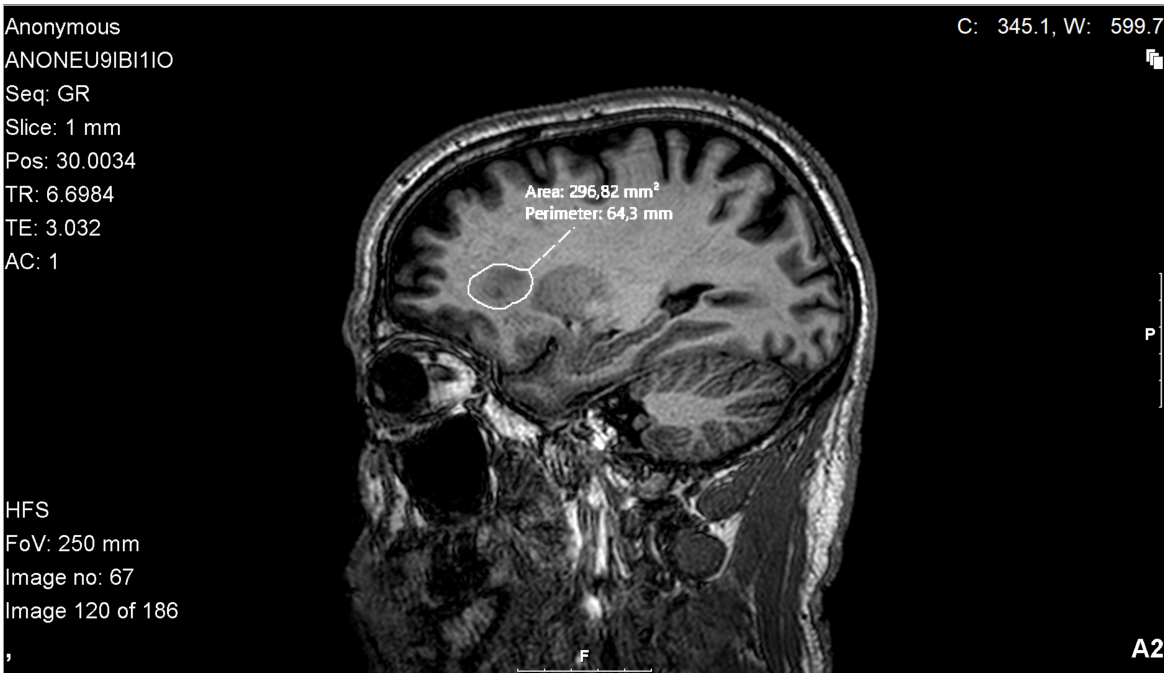

Figure 4.1: Sectra Image Viewer environment with an example of the data provided by the clinicians, showcasing a slice with a suspected FCD contour region, in a T1-weighted MRI scan.

DICOM (Digital Imaging and Communications in Medicine) is a standard protocol for managing, storing, transmitting, and printing medical images. It ensures compatibility across different imaging devices and systems, combining image data with patient information to link images with electronic health records. DICOM facilitates the exchange and sharing of medical images across various healthcare facilities and supports image compression and encryption for efficient storage and secure transmission. In MRI, DICOM is crucial for maintaining the integrity and quality of high-resolution images, managing large volumes of multi-dimensional data, and supporting advanced visualization techniques. It also integrates seamlessly with PACS, enabling radiologists and healthcare professionals to access and analyze MRI studies effectively.

Each patient's DICOM data was automatically exported into 2 folders that contained each sequence performed, T1 and FLAIR respectively, with 1 DICOM file per slice, and a third folder

where 1 DICOM file was generated for each ROI drawn. Extracting relevant information from DICOM files is done via their metadata headers, for example, each DICOM file contains the slices' pixel information stored in an array of values that range from 0 to 1, corresponding to the brightness value of each pixel, which is accessible via the header Pixel Data with the tag (7FE0,0010), a unique pair of hexadecimal values. Since MELD requires that the input MRI scans be in NIfTI format, the necessary conversion from DICOM was performed using MRICron (https://www.nitrc.org/projects/mricron), a software package used to visualize MRI scans directly in NIfTI or indirectly by converting DICOM slice folders into NIfTI.

4.2 MELD Implementation

Given MELD's reliability on FreeSurfer to extract the clinically relevant input features, a Linux-based operating system was necessary to execute the pipeline, with Ubuntu 22.04, the most recent Ubuntu distro at the start of development, being the one chosen. To maintain the goal of developing an intuitive solution to use MELD, minimizing the reliability of Ubuntu was paramount, so Windows Subsystem for Linux (WSL) was used. WSL allows the use of Linux's command-line tools within Windows, thus guaranteeing that the complete software pipeline can be used without the need to install a standalone, fully-fledged Linux operating system. Before implementing MELD, FreeSurfer version 7.2 was installed, given that it is the most recent version compatible with MELD, alongside Anaconda(108) to manage the necessary Python packages and create the programming environments. To install MELD within WSL, the steps found in their official GitHub repository (https://github.com/MELDProject/meld_classifier) were followed. MELD requires specific folders to be created, following a regimented nomenclature necessary for the correct execution of the algorithm. Every patient analyzed needs to be inserted within a folder that follows this naming scheme:"MELD_<site_code>_<scanner_field>_FCD_000X", where site_code refers to a specific ID obtained by contacting the MELD team directly, scanner_field is used to specify if the scans were obtained with an MRI machine capable of 1.5 Tesla or 3 Tesla, FCD just refers to focal cortical dysplasia and the final numbers can be chosen by the user to create unique ids. For example, a typical patient folder could be named like this: "MELD_H72_3T_FCD_0005". Inside each patient folder, two folders need to be created, one "T1" and one "FLAIR", where inside of each one the corresponding T1 and FLAIR files, in NIfTI format, are placed. Alongside

FreeSurfer and MELD, in order to merge the brain regions predicted by the algorithm with the original MRI scan, FSL (FMRIB Software Library)(109) also had to be installed. FSL is a widely used library of neuroimaging tools equipped with many functionalities, including manipulation of NIfTI brain scans.

4.3 Evaluation Method

Although the performance of the FCD detection algorithm created by MELD has been tested in multiple articles with large datasets and thorough metrics, the applicability of this method to the use case concerning the images given by the collaborating clinicians, had to be verified. To achieve this, three aspects needed to be tested:

1. Valid data format and characteristics
2. Algorithm execution
3. Output reliability

As mentioned in (105), the images acquired to train the MELD classifier were obtained from patients who performed preoperative T1-weighted and FLAIR MRI brain scans in a scanner of 1.5 or 3 Tesla, did not have any large structural abnormalities and previous brain surgery. All the images, pertaining to 22 different centers, were obtained on GE, Siemens, or Philips MRI scanners. All of these criteria are met by the data provided by Hosp. Santo António. The scans were all performed on a Philips MRI scanner with a field strength of 3 Tesla and no patient with large structural abnormalities or with previous surgeries was included. Given the correct formatting of the data, the next step was to verify if the algorithm did execute as expected. To verify this, the whole pipeline was conducted several times, with some variability inserted to check how the execution changed. Given that the algorithm can be run with just the T1 MRI scan, excluding the FLAIR, every patient was used with both scans and with just the T1. Since FreeSurfer can be used for other purposes, and generating its output is very time-consuming (about 6-7 hours), the capability of MELD to exclude the initial extraction of features, if the data is already available, was also tested, with successful results. The final step was to verify the reliability of the output, thus making sure the algorithm chosen would be a suitable option to implement within the GUI. To accomplish this, the images given by the clinicians had to be processed, in order to compare

with the results. After merging the predicted pixels with the original T1 image, the ground-truth ROIs also had to be merged with the same T1 image for comparison. One obstacle had to be overcome, as the ground truth ROIs had pixel information regarding perimeter and area that had to be removed and they were contours, not filled in regions like the predicted pixels, thus not enabling a proper performance analysis. The software GIMP(110) was used to fill the ground-truth ROIs for each slice and remove unnecessary data, with the original DICOM files being converted to PNG, edited to have the contours filled in, and re-converted to DICOM. As mentioned earlier, the ROI and T1 files are separated, and only through the Sectra Image Viewer do they appear merged. To overcome this, using the library Pydicom(111), with Python version 3.12.2, the metadata headers for each slice and ROI were analyzed to find how they were linked in Sectra Image Viewer. The header "ReferencedSOPInstanceUID" was then understood as the responsible and a script was written to automate this linking process and also to overlay the filled-in, cleaned, ground-truth ROIs with each corresponding slice in the original T1 image.

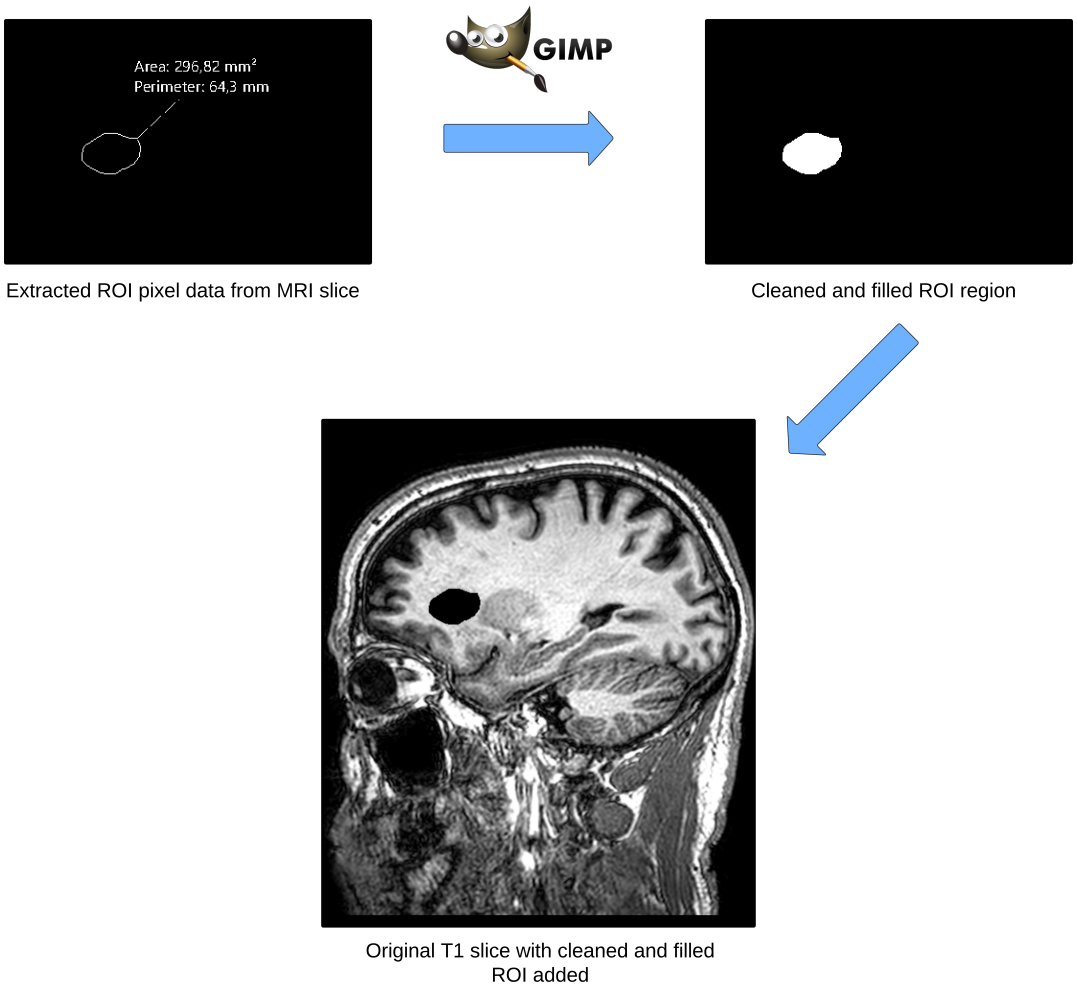

Figure 4.2: Processing pipeline for each ROI. Ground truth region in final image colored black for easier visualization.

After linking the filled-in ROIs with the correct slices, the ground-truth images were ready to be compared with the prediction. Given the limited number of patients, and the already proven clinically relevant performance from MELD, only a small number of comparisons were necessary. With the purpose being, to check the reliability of the output of the MELD classifier for the images provided.

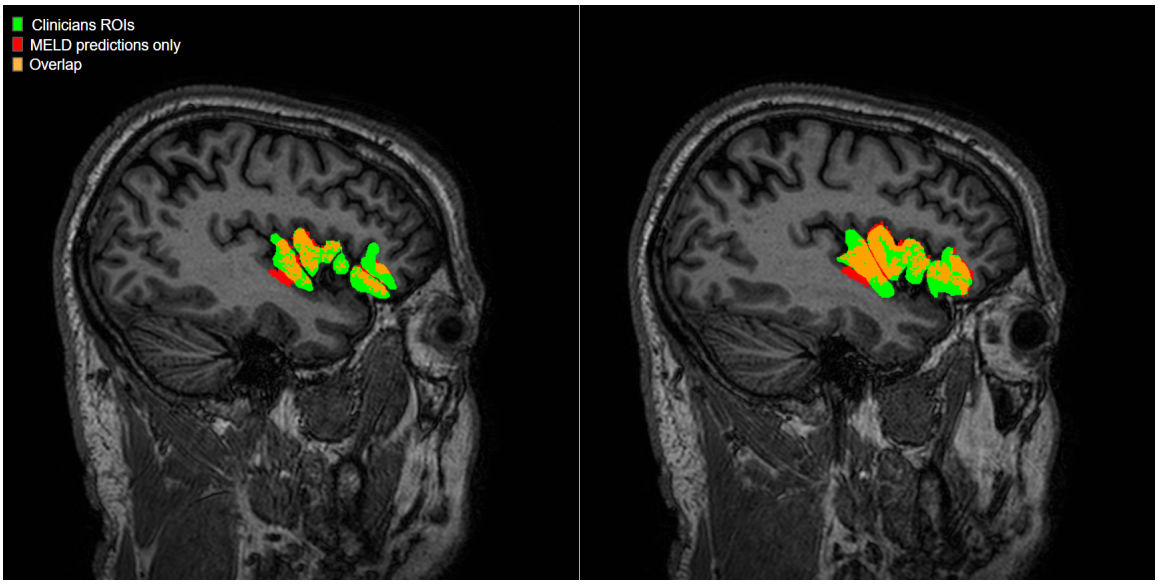

Figure 4.3: Pixel overlap of 2 different MRI slices of the same patient. Green pixels represent the ground truth clinical assessment, red pixels the predicted region, and the overlap in orange

As the images showcase, the performance expected from the method implemented by the MELD team was verified, with a very clinically relevant overlap. With all the necessary criteria being met, the next step of automating the use of this algorithm via a GUI was initiated.

4.4 GUI development

During meetings with the clinicians, it became evident that the focus should be on usability, intuitiveness, and efficiency. Their main goal was to integrate the GUI quickly into the daily clinical workflow, without having to adapt their current procedures or learn a new software stack. With this in mind, the development environment chosen was Python version 3.11 with PyQt version 4 as the GUI development kit, given the ability of this library to provide a wide variety of tools to create an efficient GUI. Alongside the main requirement of automating the execution of the prediction algorithm, a decision was made to also include some visualization features and image manipulation. This improves the user experience as the resulting prediction can be made available immediately when the output is created and within the same software, alleviating the need for clinicians to handle the files and import them to different software, thus also eliminating the risk that could arise from software incompatibilities. Ideally, it also had to run completely on Windows, at least from the perspective of the user, as adopting a new operating system like

Mac OS X or a Linux-based distribution was unfeasible. Moreover, the GUI was designed with scalability and future updates in mind. The codebase was structured to allow for easy integration of new features, improvements, and bug fixes. The GUI was then packaged as an executable file (.exe), recognized by Windows, making it ready to be distributed to the clinicians.

Chapter 5

Results and Discussion

5.1 Graphical User Interface

5.1.1 Design and Implementation

Modern GUIs have showcased a clear trend towards minimalism, with simpler interfaces restricted to the more essential functionalities, darker color palettes, and with a big focus placed on providing a pleasant experience to the user. Given that the purpose of this GUI was not just to run the prediction algorithm but also to serve extra image visualization functionalities, it had to adhere to the currently seen trend, to facilitate adoption. With this in mind, inspiration was taken from 2 different software: Visual Studio Code, given its intuitive interface, feature layout, and design choices, and MRICron, to retrieve information about which functionalities should belong in the developed GUI.

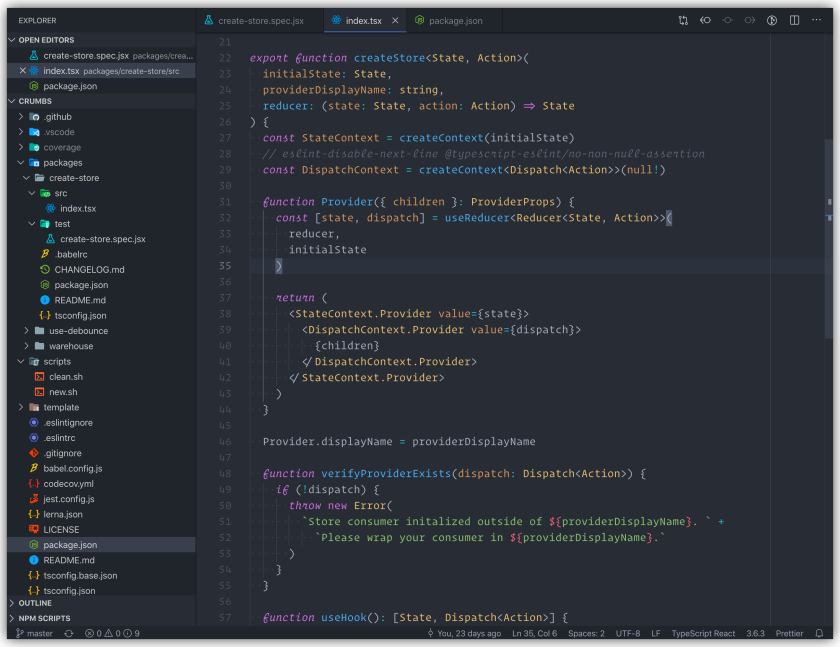

Figure 5.1: Standard Visual Studio Code interface with darker colors and an intuitive feature layout. Adapted from (112).

Figure 5.2: Screenshot taken during the use of MRICron for MRI visualization purposes.

The GUI in its current version contains a viewing area that occupies around 80% of the available space, with the capability to visualize 2 MRI images side-by-side, a file explorer on the left side, and a toolbar at the top with several options.

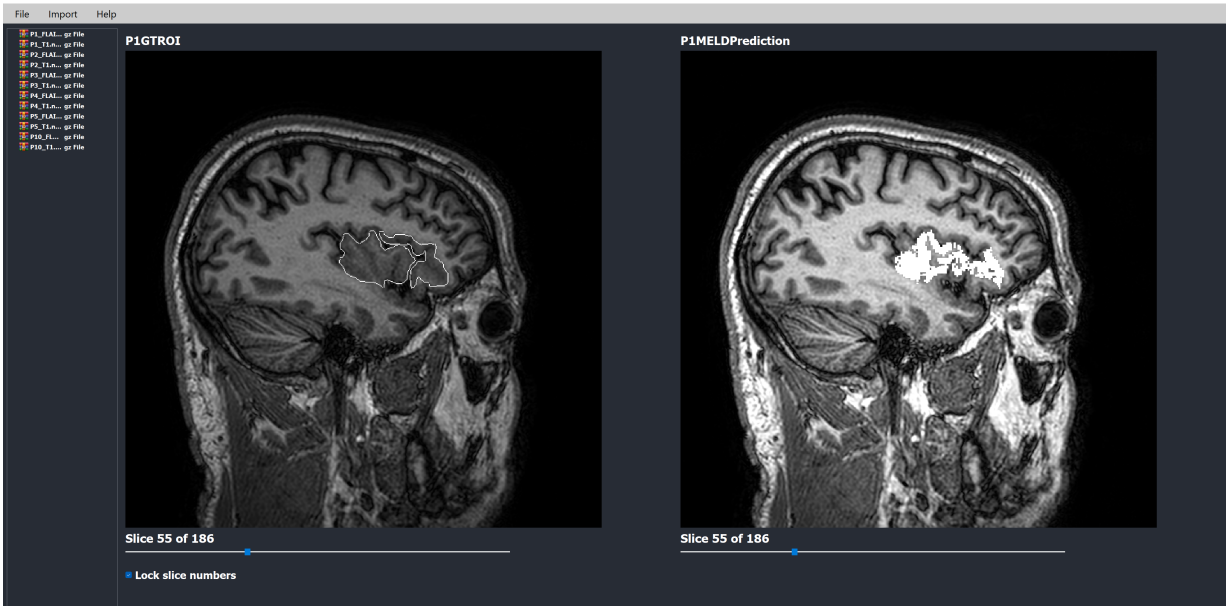

Figure 5.3: Typical GUI scenario with a ground truth ROI on the left side and a MELD prediction on the right. Both are from the same patient and with the slice numbers locked to ease navigation.

5.1.2 Feature List

When the user inputs an image, the right-click button of the mouse can be pressed over it to open a menu with different image manipulation options, useful to guarantee the specific type of visualization the user desires. These include rotating the image by 90º, flipping the image, and viewing whichever anatomical plane the user desires. Within the toolbar, the "File" menu allows the user to open a NIfTI file or a DICOM slice folder and visualize the brain scan. The user can also open a "prediction folder" that resulted from a previously run prediction, which automatically changes the file explorer location allowing for the quick input and visualization of the results. The main functionality of this GUI is also found here with the option "Run prediction...". After this is pressed, a text form popup appears, ready to receive all the relevant information to execute the algorithm from MELD.

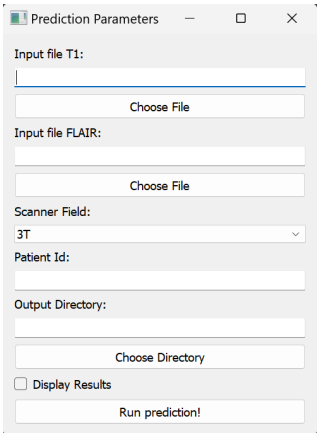

Figure 5.4: Dialog box to allow the user to input the necessary parameters to run the MELD algorithm

This is also where the user finds the recommended way to close the GUI, via the "Exit" button, as this takes into account possible processing that is still ongoing and shuts it down before closing the GUI, thus avoiding unnecessary file corruptions. The "Import" menu, is where the user finds the functionality of converting a DICOM folder into NIfTI. Given that the MELD algorithm requires that the brain scans be in NIfTI format, this was a necessary feature. Even though there are other available solutions, having this option integrated within the GUI contributes to an easy adoption. The last menu, titled "Help", has some basic information about the GUI such as its version and a small description of the various functionalities it offers.

These design choices were corroborated by the positive feedback received by the clinicians during

meetings, with a heavy emphasis being placed on the ease of use that the GUI presented, facilitating the integration of this method in the clinical workflow. Regardless, a dedicated and procedural discussion after the integration of the GUI would prove very useful, especially in finding possible bugs and improving the overall experience. Given the open-source nature of the MELD algorithm, as well as of this GUI, another possible approach could be to distribute it online. Not only does the release of GUI online quicken its development through community feedback but it also promotes cooperation among different developers and medical practitioners. The involvement of varied professionals would contribute to a deeper refinement of the GUI and a higher number of adoptions by other clinicians.

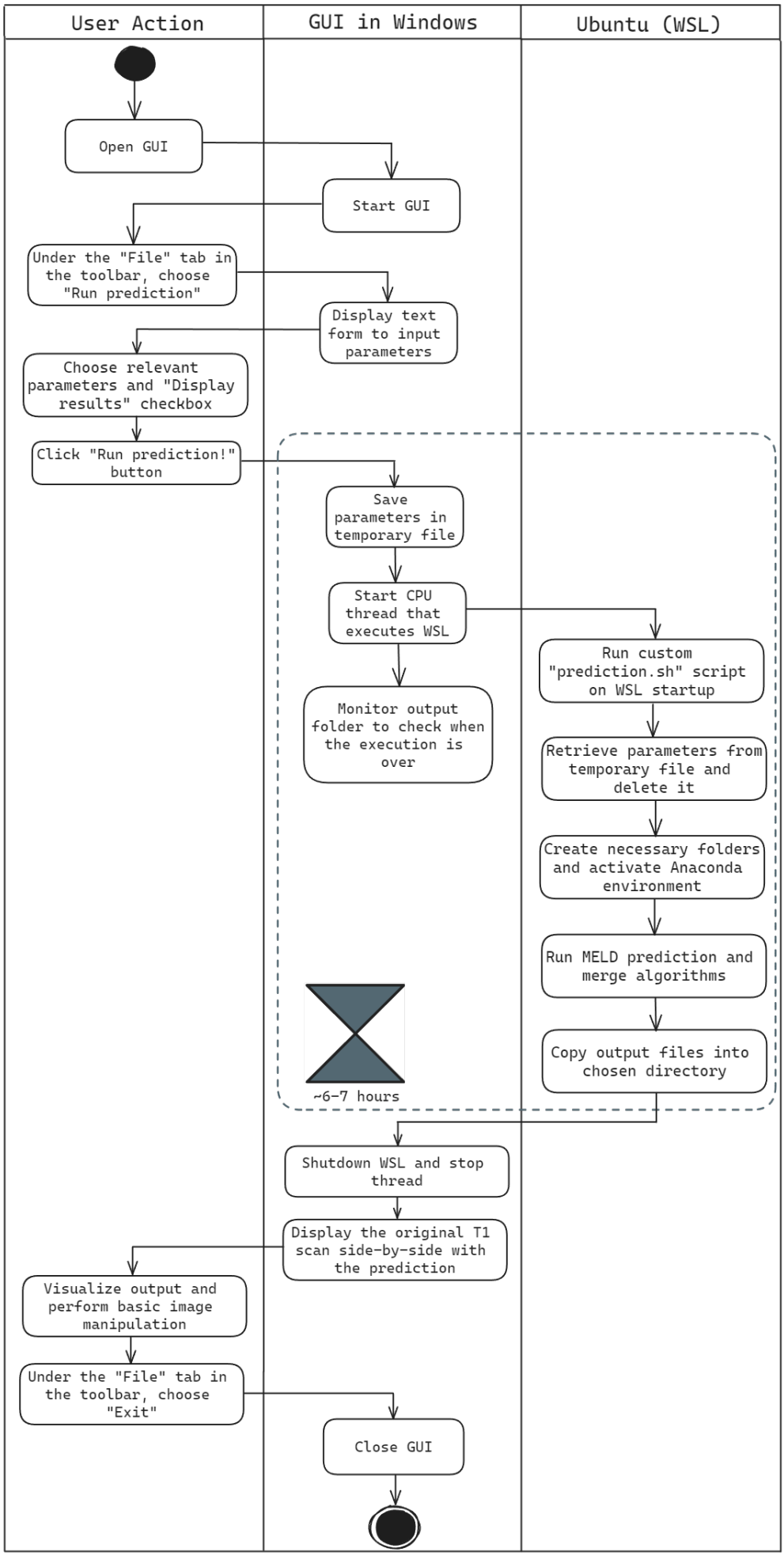

Figure 5.5: GUI use case diagram detailing the main functionality of running a prediction

Chapter 6

Conclusion

Epilepsy is a disease that has haunted humanity for thousands of years and we are still far from perfecting our clinical approach to it. For patients where antiseizure medications do not alleviate the seizures to a sustainable level, having resective surgery is often the only solution. A big emphasis is placed on the quality of the pre-surgical analysis in order to ensure the best possible clinical outcome. This process resorts to several diagnostics to properly evaluate the onset of the seizures and try to estimate a cause. If the cause is structural then it most likely is an FCD. Unfortunately, detecting FCDs by visual inspection leads to errors that could jeopardize the success of the surgery. Computer-assisted methods, both in the brain morphometry and machine learning groups, have shown very promising results but are characterized by having a steep learning curve, being difficult to implement by non-experts, and lacking a clear explanation of the reasoning behind their predictions. Although MELD has tackled the last problem, the two others create friction that reduces the number of clinicians willing to adopt these solutions and delays the eventual benefits these methods would bring to the medical world. The implementation of this GUI tries to address this at a local level, directly collaborating with clinicians who requested a solution that was easy to integrate into their daily workflow and that utilizes a prediction algorithm known to have a clinically relevant performance. This goal was achieved, and the clinical procedure of future focal refractory epilepsy patients will improve from the work developed during this dissertation.

6.1 Future Work

Although the presented solution did indeed achieve the goal proposed, there are some additional objectives that could have been accomplished.

For example, the MELD algorithm offers the possibility of adapting the parameters of its model to a given site, if provided enough images to acquire data from. This normalization procedure could improve performance as the model would assess the characteristics of the clinical environment, such as the MRI scanner used, the specific acquisition protocols, and the MRI sequences performed. Unfortunately, this procedure requires at least 30 pairs of T1/FLAIR images which was not feasible to acquire during this dissertation. Another possible improvement would be to integrate FastSurfer(113) as a replacement for FreeSurfer, effectively cutting the prediction time from around 6-7 hours to only 1 hour. This unfortunately proved to be harder than anticipated and a decision was made to guarantee the functionality of the GUI with FreeSurfer. Furthermore, a higher number of feedback sessions could have been arranged, contributing to an improved implementation of the GUI, closer to the needs presented by the clinicians.

Bibliography

[1] M. P. Kerr. The impact of epilepsy on patients' lives. *Acta Neurologica Scandinavica*, 126(s194):1–9, 2012. doi:10.1111/ane.12014.

[2] Lina Nashef, Elson L. So, Philippe Ryvlin, and Torbjörn Tomson. Unifying the definitions of sudden unexpected death in epilepsy. *Epilepsia*, 53:227–233, 2 2012. doi:10.1111/j.1528-1167.2011.03358.x.

[3] Pedro Beleza. Refractory epilepsy: A clinically oriented review. *European Neurology*, 62:65–71, 2009. doi:10.1159/000222775.

[4] Marnie T. Janson and Jacquelyn L. Bainbridge. Continuing burden of refractory epilepsy. *Annals of Pharmacotherapy*, 55:406–408, 3 2021. doi:10.1177/1060028020948056.

[5] Shu-Hao Wei and Wang-Tso Lee. Comorbidity of childhood epilepsy. *Journal of the Formosan Medical Association*, 114:1031–1038, 11 2015. doi:10.1016/j.jfma.2015.07.015.

[6] Anne M. Libby, Vahram Ghushchyan, Robert Brett McQueen, Julia F. Slejko, Jacqueline L. Bainbridge, and Jonathan D. Campbell. Economic differences in direct and indirect costs between people with epilepsy and without epilepsy. *Medical Care*, 50:928–933, 11 2012. doi:10.1097/MLR.0b013e31826c8613.

[7] Warren T. Blume. Focal and generalized: Both here and there. *Epilepsy Currents*, 10(5):115–117, September 2010. doi:10.1111/j.1535-7511.2010.01375.x.

[8] Ettore Beghi. *The Epidemiology of Epilepsy*, volume 54. S. Karger AG, 3 2020. doi:10.1159/000503831.

[9] Fergus Rugg-Gunn, Anna Miserocchi, and Andrew McEvoy. Epilepsy surgery. *Practical Neurology*, pages practneurol–2019–002192, August 2019. doi:10.1136/practneurol-2019-002192.

[10] Joanna Kabat and Przemysław Król. Focal cortical dysplasia - review. *Polish journal of radiology*, 77:35–43, 4 2012. doi:10.12659/pjr.882968.

[11] Pascal Martin, Benjamin Bender, and Niels K Focke. Post-processing of structural mri for individualized diagnostics. *Quantitative imaging in medicine and surgery*, 5:188–203, 4 2015. doi:10.3978/j.issn.2223-4292.2015.01.10.

[12] Christian G. Bien, Miriam Szinay, Jan Wagner, Hans Clusmann, Albert J. Becker, and Horst Urbach. Characteristics and surgical outcomes of patients with refractory magnetic resonance imaging–negative epilepsies. *Archives of Neurology*, 66, 12 2009. doi:10.1001/archneurol.2009.283.

[13] Zhong I. Wang, Andreas V. Alexopoulos, Stephen E. Jones, Imad M. Najm, Aleksandar Ristic, Chong Wong, Richard Prayson, Felix Schneider, Yosuke Kakisaka, Shuang Wang, William Bingaman, Jorge A. Gonzalez-Martinez, and Richard C. Burgess. Linking mri postprocessing with magnetic source imaging in mri-negative epilepsy. *Annals of Neurology*, 75:759–770, 5 2014. doi:10.1002/ana.24169.

[14] Lennart Walger, Sophie Adler, Konrad Wagstyl, Leonie Henschel, Bastian David, Valeri Borger, Elke Hattingen, Hartmut Vatter, Christian E. Elger, Torsten Baldeweg, Felix Rosenow, Horst Urbach, Albert Becker, Alexander Radbruch, Rainer Surges, Martin Reuter, Fernando Cendes, Zhong Irene Wang, Hans-Jürgen Huppertz, and Theodor Rüber. Artificial intelligence for the detection of focal cortical dysplasia: Challenges in translating algorithms into clinical practice. *Epilepsia*, 64:1093–1112, 5 2023. doi:10.1111/epi.17522.

[15] Nicola K. Dinsdale, Emma Bluemke, Vaanathi Sundaresan, Mark Jenkinson, Stephen M. Smith, and Ana I.L. Namburete. Challenges for machine learning in clinical translation of big data imaging studies. *Neuron*, 110:3866–3881, 12 2022. doi:10.1016/j.neuron.2022.09.012.

[16] Jay N Giedd, Armin Raznahan, Aaron Alexander-Bloch, Eric Schmitt, Nitin Gogtay, and Judith L Rapoport. Child psychiatry branch of the national institute of mental health longitudinal structural magnetic resonance imaging study of human brain development. *Neuropsychopharmacology*, 40:43–49, 1 2015. doi:10.1038/npp.2014.236.

[17] Simon Ducharme, Matthew D. Albaugh, Tuong-Vi Nguyen, James J. Hudziak, J.M. Mateos-Pérez, Aurelie Labbe, Alan C. Evans, and Sherif Karama. Trajectories of cortical thickness maturation in normal brain development — the importance of quality control procedures. *NeuroImage*, 125:267–279, 1 2016. doi:10.1016/j.neuroimage.2015.10.010.

[18] Sophie Adler, Konrad Wagstyl, Roxana Gunny, Lisa Ronan, David Carmichael, J Helen Cross, Paul C. Fletcher, and Torsten Baldeweg. Novel surface features for automated detection of focal cortical dysplasias in paediatric epilepsy. *NeuroImage: Clinical*, 14:18–27, 2017. doi:10.1016/j.nicl.2016.12.030.

[19] David Jiménez-Murillo, Andrés Eduardo Castro-Ospina, Leonardo Duque-Muñoz, Juan David Martínez-Vargas, Jazmín Ximena Suárez-Revelo, Jorge Mario Vélez-Arango, and Maria de la Iglesia-Vayá. Automatic detection of focal cortical dysplasia using mri: A systematic review. *Sensors*, 23:7072, 8 2023. doi:10.3390/s23167072.

[20] Christian M Kaculini, Amelia J Tate-Looney, and Ali Seifi. The history of epilepsy: From ancient mystery to modern misconception. *Cureus*, March 2021. doi:10.7759/cureus.13953.

[21] Christos P. Panteliadis, Photios Vassilyadi, Julia Fehlert, and Christian Hagel. Historical documents on epilepsy: From antiquity through the 20th century. *Brain and Development*, 39:457–463, 6 2017. doi:10.1016/j.braindev.2017.02.002.

[22] Emmanouil Magiorkinis, Kalliopi Sidiropoulou, and Aristidis Diamantis. Hallmarks in the history of epilepsy: Epilepsy in antiquity. *Epilepsy Behavior*, 17:103–108, 1 2010. doi:10.1016/j.yebeh.2009.10.023.

[23] Thomas M. Walshe. *On the Sacred Disease*. Oxford University Press, 1 2016. doi:10.1093/med/9780190218560.003.0004.

[24] Mervyn Eadie. Samuel tissot's traité de l'épilepsie —250 years old. *Journal of the History of the Neurosciences*, 28:319–331, 7 2019. doi:10.1080/0964704X.2019.1596364.

[25] V S Wong and S Y Tan. Santiago ramón y cajal (1852-1934): pride of petilla. *Singapore medical journal*, 51:683–4, 9 2010.

[26] Emmanouil Magiorkinis, Aristidis Diamantis, Kalliopi Sidiropoulou, and Christos Panteliadis. Highights in the history of epilepsy: The last 200 years. *Epilepsy Research and Treatment*, 2014:1–13, 8 2014. doi:10.1155/2014/582039.

[27] Ingrid E. Scheffer, Samuel Berkovic, Giuseppe Capovilla, Mary B. Connolly, Jacqueline French, Laura Guilhoto, Edouard Hirsch, Satish Jain, Gary W. Mathern, Solomon L. Moshé, Douglas R. Nordli, Emilio Perucca, Torbjörn Tomson, Samuel Wiebe, Yue-Hua Zhang, and Sameer M. Zuberi. scpILAE/scp classification of the epilepsies: Position paper of the scpILAE/scp commission for classification and terminology. *Epilepsia*, 58(4):512–521, March 2017. doi:10.1111/epi.13709.

[28] Sara Matricardi, Alberto Verrotti, Francesco Chiarelli, Caterina Cerminara, and Paolo Curatolo. Current advances in childhood absence epilepsy. *Pediatric Neurology*, 50(3):205–212, March 2014. doi:10.1016/j.pediatrneurol.2013.10.009.

[29] Fritz E. Dreifuss. Juvenile myoclonic epilepsy: Characteristics of a primary generalized epilepsy. *Epilepsia*, 30(s4):S1–S7, December 1989. doi:10.1111/j.1528-1157.1989.tb05832.x.

[30] Takeshi Satow, Akio Ikeda, Junichi Yamamoto, Motohiro Takayama, Masao Matsuhashi, Shinji Ohara, Riki Matsumoto, Tahamina Begum, Hidenao Fukuyama, Nobuo Hashimoto, and Hiroshi Shibasaki. Partial epilepsy manifesting atonic seizure: Report of two cases. *Epilepsia*, 43(11):1425–1431, November 2002. doi:10.1046/j.1528-1157.2002.34501.x.

[31] W. H. Theodore, R. J. Porter, P. Albert, K. Kelley, E. Bromfield, O. Devinsky, and S. Sato. The secondarily generalized tonic-clonic seizure. *Neurology*, 44(8):1403–1403, August 1994. doi:10.1212/wnl.44.8.1403.

[32] Haleema Anwar, Qudsia Umaira Khan, Natasha Nadeem, Iqra Pervaiz, Muhammad Ali, and Fatima Fayyaz Cheema. Epileptic seizures. *Discoveries*, 8:e110, 6 2020. URL: https://discoveriesjournals.org/discoveries/D.2020.02.RA-Anwar-Khan.DOI, doi:10.15190/d.2020.7.

[33] Ali H Mesiwala, John D Kuratani, Anthony M Avellino, Theodore S Roberts, Marcio A Sotero, and Richard G Ellenbogen. Focal motor seizures with secondary generalization arising in the cerebellum: case report and review of the literature. *Journal of neurosurgery*, 97(1):190–196, 2002.

[34] Robert S. Fisher. The new classification of seizures by the international league against epilepsy 2017. *Current Neurology and Neuroscience Reports*, 17(6), April 2017. doi:10.1007/s11910-017-0758-6.

[35] D. C. Taylor, M. A. Falconer, C. J. Bruton, and J. A. N. Corsellis. Focal dysplasia of the cerebral cortex in epilepsy. *Journal of Neurology, Neurosurgery &amp Psychiatry*, 34(4):369–387, August 1971. doi:10.1136/jnnp.34.4.369.

[36] Ingmar Blümcke, Maria Thom, Eleonora Aronica, Dawna D. Armstrong, Harry V. Vinters, Andre Palmini, Thomas S. Jacques, Giuliano Avanzini, A. James Barkovich, Giorgio Battaglia, Albert Becker, Carlos Cepeda, Fernando Cendes, Nadia Colombo, Peter Crino, J. Helen Cross, Olivier Delalande, François Dubeau, John Duncan, Renzo Guerrini, Philippe Kahane, Gary Mathern, Imad Najm, Çiğdem Özkara, Charles Raybaud, Alfonso Represa, Steven N. Roper, Noriko Salamon, Andreas Schulze-Bonhage, Laura Tassi, Annamaria Vezzani, and Roberto Spreafico. The clinicopathologic spectrum of focal cortical dysplasias: A consensus classification proposed by an ad hoc task force of the ILAE diagnostic methods commission1. *Epilepsia*, 52(1):158–174, November 2010. doi:10.1111/j.1528-1167.2010.02777.x.

[37] L. E. Jeha, I. Najm, W. Bingaman, D. Dinner, P. Widdess-Walsh, and H. Luders. Surgical outcome and prognostic factors of frontal lobe epilepsy surgery. *Brain*, 130(2):574–584, February 2007. doi:10.1093/brain/awl364.

[38] Erica C. Sá de Camargo and Walter J. Koroshetz. Neuroimaging of ischemia and infarction. *NeuroRX*, 2:265–276, 4 2005. doi:10.1602/neurorx.2.2.265.

[39] Mark A King, Mark R Newton, Graeme D Jackson, Gregory J Fitt, L Anne Mitchell, Mervyn J Silvapulle, and Samuel F Berkovic. Epileptology of the first-seizure presentation: a clinical, electroencephalographic, and magnetic resonance imaging study of 300 consecutive patients. *The Lancet*, 352:1007–1011, 9 1998. doi:10.1016/S0140-6736(98)03543-0.

[40] N Salamon, J Kung, S J Shaw, J Koo, S Koh, J Y Wu, J T Lerner, R Sankar, W D Shields, J Engel, I Fried, H Miyata, W H Yong, H V Vinters, and G W Mathern. Fdg-pet/mri coregistration improves detection of cortical dysplasia in patients with epilepsy. *Neurology*, 71:1594–601, 11 2008. doi:10.1212/01.wnl.0000334752.41807.2f.

[41] Masaki IWASAKI, Kazutaka JIN, Nobukazu NAKASATO, and Teiji TOMINAGA. Non-invasive evaluation for epilepsy surgery. *Neurologia medico-chirurgica*, 56:632–640, 2016. doi:10.2176/nmc.ra.2016-0186.

[42] Fernando Cendes, William H. Theodore, Benjamin H. Brinkmann, Vlastimil Sulc, and Gregory D. Cascino. *Neuroimaging of epilepsy*, pages 985–1014. 2016. doi:10.1016/B978-0-444-53486-6.00051-X.

[43] S Chan, J K Erickson, and S S Yoon. Limbic system abnormalities associated with mesial temporal sclerosis: a model of chronic cerebral changes due to seizures. *Radiographics : a review publication of the Radiological Society of North America, Inc*, 17:1095–110, 1997. doi:10.1148/radiographics.17.5.9308104.

[44] Gregory D Cascino, Joseph I Sirven, and William O Tatum, editors. *Epilepsy*. Wiley, 6 2021. doi:10.1002/9781119431893.

[45] Nadia Colombo, Laura Tassi, Francesco Deleo, Alberto Citterio, Manuela Bramerio, Roberto Mai, Ivana Sartori, Francesco Cardinale, Giorgio Lo Russo, and Roberto Spreafico. Focal cortical dysplasia type iia and iib: Mri aspects in 118 cases proven by histopathology. *Neuroradiology*, 54:1065–1077, 10 2012. doi:10.1007/s00234-012-1049-1.

[46] Bo Jin, Jing Wang, Jian Zhou, Shuang Wang, Yuguang Guan, and Shuhua Chen. A longitudinal study of surgical outcome of pharmacoresistant epilepsy caused by focal

cortical dysplasia. *Journal of Neurology*, 263:2403–2410, 12 2016. doi:10.1007/s00415-016-8274-1.

[47] Siobhan West, Sarah J Nevitt, Jennifer Cotton, Sacha Gandhi, Jennifer Weston, Ajay Sudan, Roberto Ramirez, and Richard Newton. Surgery for epilepsy. *The Cochrane database of systematic reviews*, 6:CD010541, 6 2019. doi:10.1002/14651858.CD010541.pub3.

[48] H Haug. History of neuromorphometry. *Journal of neuroscience methods*, 18:1–17, 10 1986. doi:10.1016/0165-0270(86)90110-x.

[49] Arne May and Christian Gaser. Magnetic resonance-based morphometry: a window into structural plasticity of the brain. *Current Opinion in Neurology*, 19:407–411, 8 2006. doi:10.1097/01.wco.0000236622.91495.21.

[50] John Ashburner and Karl J. Friston. Voxel-based morphometry—the methods. *NeuroImage*, 11:805–821, 6 2000. doi:10.1006/nimg.2000.0582.

[51] Geraldo F Busatto, Breno S Diniz, and Marcus V Zanetti. Voxel-based morphometry in alzheimer's disease. *Expert Review of Neurotherapeutics*, 8:1691–1702, 11 2008. doi:10.1586/14737175.8.11.1691.

[52] Aino I L Saarinen, Sanna Huhtaniska, Juho Pudas, Lassi Björnholm, Tuomas Jukuri, Jussi Tohka, Niklas Granö, Jennifer H Barnett, Vesa Kiviniemi, Juha Veijola, Mirka Hintsanen, and Johannes Lieslehto. Structural and functional alterations in the brain gray matter among first-degree relatives of schizophrenia patients: A multimodal meta-analysis of fmri and vbm studies. *Schizophrenia research*, 216:14–23, 2 2020. doi:10.1016/j.schres.2019.12.023.

[53] Miaomiao Yu, Xinyu Gao, Xiaoyu Niu, Mengzhe Zhang, Zhengui Yang, Shaoqiang Han, Jingliang Cheng, and Yong Zhang. Meta-analysis of structural and functional alterations of brain in patients with attention-deficit/hyperactivity disorder. *Frontiers in psychiatry*, 13:1070142, 2022. doi:10.3389/fpsyt.2022.1070142.

[54] Clarissa Lin Yasuda, Luiz Eduardo Betting, and Fernando Cendes. Voxel-based morphometry and epilepsy. *Expert review of neurotherapeutics*, 10:975–84, 6 2010. doi:10.1586/ern.10.63.

[55] Stephen M. Smith. Fast robust automated brain extraction. *Human Brain Mapping*, 17:143–155, 11 2002. doi:10.1002/hbm.10062.

[56] D W Shattuck, S R Sandor-Leahy, K A Schaper, D A Rottenberg, and R M Leahy. Magnetic resonance image tissue classification using a partial volume model. *NeuroImage*, 13:856–76, 5 2001. doi:10.1006/nimg.2000.0730.

[57] Andrew Hoopes, Jocelyn S Mora, Adrian V Dalca, Bruce Fischl, and Malte Hoffmann. Synthstrip: skull-stripping for any brain image. *NeuroImage*, 260:119474, 10 2022. doi:10.1016/j.neuroimage.2022.119474.

[58] Linmin Pei, Murat Ak, Nourel Hoda M Tahon, Serafettin Zenkin, Safa Alkarawi, Abdallah Kamal, Mahir Yilmaz, Lingling Chen, Mehmet Er, Nursima Ak, and Rivka Colen. A general skull stripping of multiparametric brain mris using 3d convolutional neural network. *Scientific reports*, 12:10826, 6 2022. doi:10.1038/s41598-022-14983-4.

[59] J G Sled, A P Zijdenbos, and A C Evans. A nonparametric method for automatic correction of intensity nonuniformity in mri data. *IEEE transactions on medical imaging*, 17:87–97, 2 1998. doi:10.1109/42.668698.

[60] Marco Ganzetti, Nicole Wenderoth, and Dante Mantini. Quantitative evaluation of intensity inhomogeneity correction methods for structural mr brain images. *Neuroinformatics*, 14:5–21, 1 2016. doi:10.1007/s12021-015-9277-2.

[61] John Ashburner and Karl J. Friston. Unified segmentation. *NeuroImage*, 26:839–851, 7 2005. doi:10.1016/j.neuroimage.2005.02.018.

[62] Y. Zhang, M. Brady, and S. Smith. Segmentation of brain mr images through a hidden markov random field model and the expectation-maximization algorithm. *IEEE Transactions on Medical Imaging*, 20:45–57, 2001. doi:10.1109/42.906424.

[63] Nicholas J Tustison, Brian B Avants, Philip A Cook, Yuanjie Zheng, Alexander Egan, Paul A Yushkevich, and James C Gee. N4itk: improved n3 bias correction. *IEEE transactions on medical imaging*, 29:1310–20, 6 2010. doi:10.1109/TMI.2010.2046908.

[64] N. Tzourio-Mazoyer, B. Landeau, D. Papathanassiou, F. Crivello, O. Etard, N. Delcroix, B. Mazoyer, and M. Joliot. Automated anatomical labeling of activations in spm using a macroscopic anatomical parcellation of the mni mri single-subject brain. *NeuroImage*, 15:273–289, 1 2002. doi:10.1006/nimg.2001.0978.

[65] J. Komatsu, I. Matsunari, M. Samuraki, K. Shima, M. Noguchi-Shinohara, K. Sakai, T. Hamaguchi, K. Ono, H. Matsuda, and M. Yamada. Optimization of dartel settings for the detection of alzheimer disease. *American Journal of Neuroradiology*, 39:473–478, 3 2018. doi:10.3174/ajnr.A5509.

[66] D JONES, M SYMMS, M CERCIGNANI, and R HOWARD. The effect of filter size on vbm analyses of dt-mri data. *NeuroImage*, 26:546–554, 6 2005. doi:10.1016/j.neuroimage.2005.02.013.

[67] Cristina Scarpazza, Stefania Tognin, Silvia Frisciata, Giuseppe Sartori, and Andrea Mechelli. False positive rates in voxel-based morphometry studies of the human brain: Should we be worried? *Neuroscience Biobehavioral Reviews*, 52:49–55, 5 2015. doi:10.1016/j.neubiorev.2015.02.008.

[68] Chenyi Yu, Yuchuan Fu, Yi Lu, Yinyin Huang, Fangfang Chen, Jiayun Wei, Lingling Li, Janet Akoto Ampadu, Yu Wang, Weikun Zheng, Changcan Jiang, Weiyuan Li, Su Lui, and Xiaohong Cai. Alterations of brain gray matter volume in children with obstructive sleep apnea. *Frontiers in neurology*, 14:1107086, 2023. doi:10.3389/fneur.2023.1107086.

[69] Ali K Bourisly, Ahmed El-Beltagi, Jigi Cherian, Grace Gejo, Abrar Al-Jazzaf, and Mohammad Ismail. A voxel-based morphometric magnetic resonance imaging study of the brain detects age-related gray matter volume changes in healthy subjects of 21–45 years old. *The Neuroradiology Journal*, 28:450–459, 10 2015. doi:10.1177/1971400915598078.

[70] Alessia Sarica, Andrea Quattrone, Marianna Crasà, Rita Nisticò, Maria Grazia Vaccaro, Maria Giovanna Bianco, Vera Gramigna, Marida De Maria, Basilio Vescio, Federico Rocca, and Aldo Quattrone. Cerebellar voxel-based morphometry in essential tremor. *Journal of Neurology*, 269:6029–6035, 11 2022. doi:10.1007/s00415-022-11291-9.

[71] Thomas Nichols and Satoru Hayasaka. Controlling the familywise error rate in functional neuroimaging: a comparative review. *Statistical Methods in Medical Research*, 12:419–446, 10 2003. doi:10.1191/0962280203sm341ra.

[72] Leonardo Bonilha, Maria Augusta Montenegro, Chris Rorden, Gabriela Castellano, Marilisa Mantovani Guerreiro, Fernando Cendes, and Li Min Li. Voxel-based morphometry reveals excess gray matter concentration in patients with focal cortical dysplasia. *Epilepsia*, 47:908–15, 5 2006. doi:10.1111/j.1528-1167.2006.00548.x.

[73] Z. Irene Wang, Stephen E. Jones, Zeenat Jaisani, Imad M. Najm, Richard A. Prayson, Richard C. Burgess, Balu Krishnan, Aleksandar Ristic, Chong H. Wong, William Bingaman, Jorge A. Gonzalez-Martinez, and Andreas V. Alexopoulos. Voxel-based morphometric magnetic resonance imaging (mri) postprocessing in mri -negative epilepsies. *Annals of Neurology*, 77:1060–1075, 6 2015. doi:10.1002/ana.24407.

[74] Yilin Zhao, Jieqiong Lin, Xinxin Qi, Dezhi Cao, Fengjun Zhu, Li Chen, Zeshi Tan, Tong Mo, and Hongwu Zeng. To explore the potential mechanisms of cognitive impairment in children with mri-negative pharmacoresistant epilepsy due to focal cortical dysplasia: A pilot study from gray matter structure view. *Heliyon*, 10:e26609, 2 2024. doi:10.1016/j.heliyon.2024.e26609.

[75] Shan Shen, Andre J. Szameitat, and Annette Sterr. Vbm lesion detection depends on the normalization template: a study using simulated atrophy. *Magnetic Resonance Imaging*, 25:1385–1396, 12 2007. doi:10.1016/j.mri.2007.03.025.

[76] M. Goto, O. Abe, S. Aoki, N. Hayashi, T. Miyati, H. Takao, H. Matsuda, F. Yamashita, T. Iwatsubo, H. Mori, A. Kunimatsu, K. Ino, K. Yano, and K. Ohtomo. Influence of parameter settings in voxel-based morphometry 8. *Methods of Information in Medicine*, 54:171–178, 1 2015. doi:10.3414/ME14-01-0049.

[77] Thomas W Allan, Julien Besle, Dave R M Langers, Jeff Davies, Deborah A Hall, Alan R Palmer, and Peyman Adjamian. Neuroanatomical alterations in tinnitus assessed with magnetic resonance imaging. *Frontiers in aging neuroscience*, 8:221, 2016. doi:10.3389/fnagi.2016.00221.

[78] Keita Sakurai, Daita Kaneda, Satoru Morimoto, Yuto Uchida, Shohei Inui, Yasuyuki Kimura, Hirohito Kan, Takashi Kato, Kengo Ito, and Yoshio Hashizume. Voxel-based and surface-based morphometry analysis in patients with pathologically confirmed argyrophilic grain disease and alzheimer's disease. *Journal of Alzheimer's Disease*, 93:379–387, 5 2023. doi:10.3233/JAD-230068.

[79] Hosung Kim, Ji-Hoon Kim, Katherine L Possin, Joseph Winer, Michael D Geschwind, Duan Xu, and Christopher P Hess. Surface-based morphometry reveals caudate subnuclear structural damage in patients with premotor huntington disease. *Brain imaging and behavior*, 11:1365–1372, 10 2017. doi:10.1007/s11682-016-9616-4.

[80] Cornelius Kronlage, Ev-Christin Heide, Gisela E Hagberg, Benjamin Bender, Klaus Scheffler, Pascal Martin, and Niels Focke. Mp2rage vs. mprage surface-based morphometry in focal epilepsy. *PloS one*, 19:e0296843, 2024. doi:10.1371/journal.pone.0296843.

[81] Zhengzhen Li, Jingjing Zhang, Fuqin Wang, Yang Yang, Jie Hu, Qinghui Li, Maoqiang Tian, Tonghuan Li, Bingsheng Huang, Heng Liu, and Tijiang Zhang. Surface-based morphometry study of the brain in benign childhood epilepsy with centrotemporal spikes. *Annals of translational medicine*, 8:1150, 9 2020. doi:10.21037/atm-20-5845.

[82] Tianhong Wang, Yanli Zhang, Jiang Nan, Jianlin Li, Junqiang Lei, and Shunlin Guo. Surface-based morphometry study of brain in patients with carbon monoxide poisoning. *European journal of radiology*, 160:110711, 3 2023. doi:10.1016/j.ejrad.2023.110711.

[83] A M Dale, B Fischl, and M I Sereno. Cortical surface-based analysis. i. segmentation and surface reconstruction. *NeuroImage*, 9:179–94, 2 1999. doi:10.1006/nimg.1998.0395.

[84] Douglas N Greve and Bruce Fischl. False positive rates in surface-based anatomical analysis. *NeuroImage*, 171:6–14, 5 2018. doi:10.1016/j.neuroimage.2017.12.072.

[85] Kenia Martínez and Roberto Colom. *Imaging the Intelligence of Humans*, pages 44–69. Cambridge University Press, 5 2021. doi:10.1017/9781108635462.005.

[86] Horst Urbach, Björn Scheffler, Thomas Heinrichsmeier, Joachim VonOertzen, Thomas Kral, Joerg Wellmer, Johannes Schramm, OtmarD. Wiestler, and Ingmar Blümcke. Focal cortical dysplasia of taylor's balloon cell type: A clinicopathological entity with characteristic neuroimaging and histopathological features, and favorable postsurgical outcome. *Epilepsia*, 43:33–40, 1 2002. doi:10.1046/j.1528-1157.2002.38201.x.

[87] Peter Widdess-Walsh, Beate Diehl, and Imad Najm. Neuroimaging of focal cortical dysplasia. *Journal of Neuroimaging*, 16:185–196, 7 2006. doi:10.1111/j.1552-6569.2006.00025.x.

[88] Zohreh Ganji, Mohsen Aghaee Hakak, Seyed Amir Zamanpour, and Hoda Zare. Automatic detection of focal cortical dysplasia type ii in mri: Is the application of surface-based morphometry and machine learning promising? *Frontiers in Human Neuroscience*, 15, 2 2021. doi:10.3389/fnhum.2021.608285.

[89] Iqbal H. Sarker. Machine learning: Algorithms, real-world applications and research directions. *SN Computer Science*, 2:160, 5 2021. doi:10.1007/s42979-021-00592-x.

[90] Rahul C Deo. Machine learning in medicine. *Circulation*, 132:1920–30, 11 2015. doi:10.1161/CIRCULATIONAHA.115.001593.

[91] Jae-Hwan Kang, Yoon Gi Chung, and Sung-Phil Kim. An efficient detection of epileptic seizure by differentiation and spectral analysis of electroencephalograms. *Computers in biology and medicine*, 66:352–6, 11 2015. doi:10.1016/j.compbiomed.2015.04.034.

[92] Imran Goker, Onur Osman, Serhat Ozekes, M Baris Baslo, Mustafa Ertas, and Yekta Ulgen. Classification of juvenile myoclonic epilepsy data acquired through scanning electromyography with machine learning algorithms. *Journal of medical systems*, 36:2705–11, 10 2012. doi:10.1007/s10916-011-9746-6.

[93] Seok-Jun Hong, Boris C Bernhardt, Dewi S Schrader, Neda Bernasconi, and Andrea Bernasconi. Whole-brain mri phenotyping in dysplasia-related frontal lobe epilepsy. *Neurology*, 86:643–50, 2 2016. doi:10.1212/WNL.0000000000002374.

[94] Huiquan Wang, S. Nizam Ahmed, and Mrinal Mandal. Automated detection of focal cortical dysplasia using a deep convolutional neural network. *Computerized Medical Imaging and Graphics*, 79:101662, 1 2020. doi:10.1016/j.compmedimag.2019.101662.

[95] Ravnoor Singh Gill, Hyo-Min Lee, Benoit Caldairou, Seok-Jun Hong, Carmen Barba, Francesco Deleo, Ludovico D'Incerti, Vanessa Cristina Mendes Coelho, Matteo Lenge, Mira Semmelroch, et al. Multicenter validated detection of focal cortical dysplasia using deep learning. *Neurology*, 2021. doi:10.1212/WNL.0000000000012698.

[96] Bilal Ahmed, Carla E Brodley, Karen E Blackmon, Ruben Kuzniecky, Gilad Barash, Chad Carlson, Brian T Quinn, Werner Doyle, Jacqueline French, Orrin Devinsky, and Thomas Thesen. Cortical feature analysis and machine learning improves detection of "mri-negative" focal cortical dysplasia. *Epilepsy behavior : EB*, 48:21–8, 7 2015. doi:10.1016/j.yebeh.2015.04.055.

[97] J. Wagner, B. Weber, H. Urbach, C. E. Elger, and H.-J. Huppertz. Morphometric mri analysis improves detection of focal cortical dysplasia type ii. *Brain*, 134:2844–2854, 10 2011. doi:10.1093/brain/awr204.

[98] Statistical parametric mapping. https://www.fil.ion.ucl.ac.uk/spm/. Accessed: 2024-06-20.

[99] Computational anatomy toolbox (cat). http://www.neuro.uni-jena.de/cat/. Accessed: 2024-06-20.

[100] Advanced normalization tools (ants). http://stnava.github.io/ANTs/. Accessed: 2024-06-20.

[101] Brainvisa. http://brainvisa.info/. Accessed: 2024-06-20.

[102] Civet. http://www.bic.mni.mcgill.ca/ServicesSoftware/CIVET. Accessed: 2024-06-20.

[103] Freesurfer. https://surfer.nmr.mgh.harvard.edu/. Accessed: 2024-06-20.

[104] Ruslan Aliev, Ekaterina Kondrateva, Maxim Sharaev, Oleg Bronov, Alexey Marinets, Sergey Subbotin, Alexander Bernstein, and Evgeny Burnaev. Convolutional neural networks for automatic detection of focal cortical dysplasia. 10 2020.

[105] Hannah Spitzer, Mathilde Ripart, Kirstie Whitaker, Felice D'Arco, Kshitij Mankad, Andrew A Chen, Antonio Napolitano, Luca De Palma, Alessandro De Benedictis, Stephen Foldes, Zachary Humphreys, Kai Zhang, Wenhan Hu, Jiajie Mo, Marcus Likeman, Shirin Davies, Christopher Güttler, Matteo Lenge, Nathan T Cohen, Yingying Tang, Shan Wang, Aswin Chari, Martin Tisdall, Nuria Bargallo, Estefanía Conde-Blanco, Jose Carlos Pariente, Saül Pascual-Diaz, Ignacio Delgado-Martínez, Carmen Pérez-Enríquez, Ilaria Lagorio, Eugenio Abela, Nandini Mullatti, Jonathan O'Muircheartaigh, Katy Vecchiato, Yawu Liu, Maria Eugenia Caligiuri, Ben Sinclair, Lucy Vivash, Anna Willard, Jothy Kandasamy, Ailsa McLellan, Drahoslav Sokol, Mira Semmelroch, Ane G Kloster, Giske Opheim, Letícia Ribeiro, Clarissa Yasuda, Camilla Rossi-Espagnet, Khalid Hamandi, Anna Tietze, Carmen Barba, Renzo Guerrini, William Davis Gaillard, Xiaozhen You, Irene Wang, Sofía González-Ortiz, Mariasavina Severino, Pasquale Striano, Domenico Tortora, Reetta Kälviäinen, Antonio Gambardella, Angelo Labate, Patricia Desmond, Elaine Lui, Terence O'Brien, Jay Shetty, Graeme Jackson, John S Duncan, Gavin P Winston, Lars H Pinborg, Fernando Cendes, Fabian J Theis, Russell T Shinohara, J Helen Cross, Torsten Baldeweg, Sophie Adler, and Konrad Wagstyl. Interpretable surface-based detection of focal cortical dysplasias: a multi-centre epilepsy lesion detection study. *Brain*, 145:3859–3871, 11 2022. doi:10.1093/brain/awac224.

[106] Jean-Philippe Fortin, Nicholas Cullen, Yvette I Sheline, Warren D Taylor, Irem Aselcioglu, Philip A Cook, Phil Adams, Crystal Cooper, Maurizio Fava, Patrick J McGrath, Melvin McInnis, Mary L Phillips, Madhukar H Trivedi, Myrna M Weissman, and Russell T Shinohara. Harmonization of cortical thickness measurements across scanners and sites. *NeuroImage*, 167:104–120, 2 2018. doi:10.1016/j.neuroimage.2017.11.024.

[107] Mukund Sundararajan, Ankur Taly, and Qiqi Yan. Axiomatic attribution for deep networks. 3 2017.

[108] Anaconda software distribution, 2020. URL: https://docs.anaconda.com/.

[109] Mark Jenkinson, Christian F. Beckmann, Timothy E.J. Behrens, Mark W. Woolrich, and Stephen M. Smith. Fsl. *NeuroImage*, 62:782–790, 8 2012. doi:10.1016/j.neuroimage.2011.09.015.

[110] The GIMP Development Team. Gimp. URL: https://www.gimp.org.

[111] D. L. Mason et al. pydicom: An open source dicom library. https://github.com/pydicom/pydicom. Online; accessed YYYY-MM-DD.

[112] One Dark. vscode-one-dark-theme. https://github.com/one-dark/vscode-one-dark-theme. Accessed: 2024-06-20.

[113] Leonie Henschel, Sailesh Conjeti, Santiago Estrada, Kersten Diers, Bruce Fischl, and Martin Reuter. Fastsurfer - a fast and accurate deep learning based neuroimaging pipeline. *NeuroImage*, 219:117012, 10 2020. doi:10.1016/j.neuroimage.2020.117012.